Reactivity Studies of Chelated Maleate Ion: Stereoselectivity and Structural Correlations

Anders Hammershøi,[1] Alan M. Sargeson,* and William L. Steffen[2]

Contribution from the Research School of Chemistry, The Australian National University, Canberra, A.C.T. 2600, Australia. *Received July 20, 1983*

Abstract: [Bis(1,2-ethanediamine)(maleato)]cobalt(III) ion (Λ-[Co(en)$_2$(maleato)]$^+$ (**1**)) undergoes parallel OH^- catalyzed reactions in aqueous solutions, first order in [OH^-], to give stereospecific addition of a 2-aminoethaneaminato ion at the chelated olefin center and thereby (*R*)-*N*-(2-aminoethyl)aspartate (*R*-aea) bound as a quadridentate in Λ-*mer*(5,5)-[Co(en)(*R*-aea)]$^+$ (**3**) (k = 0.09 M^{-1} s^{-1}, 25 °C, μ = 1 M). The other path (k = 0.36 M^{-1} s^{-1}) produced *cis*- and *trans*-[Co(en)$_2$(OH)(maleato)] complexes (**19**, **20**) where the ring-opened monodentate ligand is unreactive. Similar stereoselectivity was observed for the reaction in liquid NH_3 and dimethyl sulfoxide without ring opening. Equilibrium studies established that the *fac*(5,5)-[Co(en)(aea)]$^+$ isomer was more stable (96%) than the mer isomer (4%) produced by kinetic control. In the alkaline conditions the mer isomer also dissociates a carboxylate group and isomerizes about the cobalt center. The kinetics of this process were also followed. X-ray crystallographic analyses of the Λ-[Co(en)$_2$(maleato)]PF_6·2H_2O (I), racemic [Co(en)(aea)(H_2O)]ClO_4·2H_2O (II), and Δ-*fac*(5,5)-[Co(en)(aea)]BCS·3H_2O (III) (BCS^- = (+)$_{589}$-α-bromocamphorsulfonate anion) salts were carried out to determine their connectivities and absolute configurations by the anomalous dispersion method. For I: space group $P2_1$; a = 11.629 (6) Å, b = 7.701 (4) Å, c = 9.379 (4) Å, β = 97.18 (1)°, Z = 2, 4336 reflections ($F^2 \geq 3.0\sigma(F^2)$), residual R_1 = 0.045. For II: space group $P2_1/c$; a = 7.191 (1) Å, b = 10.915 (2) Å, c = 20.723 (6) Å, β = 91.41 (1)°, Z = 4, 4796 reflections ($F^2 \geq 3.0\sigma(F^2)$), residual R_1 = 0.045. For III: space group $P1$; a = 6.976 (1) Å, b = 7.242 (1) Å, c = 14.248 (2) Å, α = 76.89 (1)°, β = 84.61 (1)°, γ = 70.86 (1)°, Z = 1, 4731 reflections ($F^2 \geq 3.0\sigma(F^2)$), residual R_1 = 0.040. The absolute configuration of the complex cation was also deduced from that of the BCS^- anion. The chiral *N*-(2-aminoethyl)aspartate was biologically inactive in an aspergillomarasmine sense, but the results in general provide some support for Glusker's "ferrous wheel" mechanism for aconitase.

The enzyme aconitase catalyzes the inverconversion of citrate via *cis*-aconitate to (2*R*,3*S*)-isocitrate, this process being part of the respiratory citric acid cycle.[3] The purified enzyme contains iron (~3 atoms/molecule of enzyme) and requires at least some of it in a reduced form for activity.[4] This observation in addition to the well-known complexing ability of at least two of the substrates led to the assumption that the overall process catalyzed by aconitase involves binding of substrate to iron bound in the enzyme.[5] This picture of the binding situation is also consistent with other experimental findings.[5,6] A detailed mechanism, referred to as the "ferrous wheel" mechanism, has been proposed and defended by Glusker.[7] The proposal is to a large degree based on the results from extensive studies of the conformational characteristics of citrate, *cis*-aconitate, and (2*R*,3*S*)-isocitrate in crystal structures of each of these anions with various cations.[5] The suggested mechanism appears to be consistent with the present knowledge about the organic chemistry of aconitase, its substrates, and known inhibitors. However, based almost entirely as it is on structural information, the proposal does not at present offer support for the reactivity aspects implied by the mechanism. *cis*-Aconitate is proposed to coordinate to the metal center with two carboxylate groups forming a seven-membered chelate ring, which includes the carbon–carbon double bond. Hydration of this double bond, to give either citrate or isocitrate, is then initiated by attack on the alkene of hydroxide ion coordinated to the same metal center. However, it is generally known that nucleophilic attack on isolated carbon–carbon double bonds usually is not very facile unless the double bond is somehow activated by polarization.[8] Such activation is effected by adjacent electron-withdrawing substituents or substituents, which through conjugation with the olefin π-electron system can assist in stabilizing the developing carbanion.[8] For example, in maleate dimethyl ester the olefin bond is indeed activated to allow attack by an amine,[9] whereas the maleate dianion does not react,[10] presumably due to donation of electron density into the alkene bond by the carboxylate anions. Taking maleate as a model for *cis*-aconitate, it is not yet clear if binding of the maleate dianion to a metal center would modify the reactivity of the double bond toward attack by a nucleophile. We find that a clarification on this point is important for further justification of Glusker's proposal. The present study was motivated in part by this argument and also by a more general need to explore the reactivity of coordinated organic molecules and the manner in which the metal ion can modify reactivity.

Amine complexes of Co(III) have been chosen to support the substrate because these complexes are robust and relatively kinetically inert to dissociation of their ligands. Such properties allow the routes for the ligand reactions to be examined in some detail free of the complications of ligand/metal ion dissociation phenomena. Thereby the efficacy of different paths for reactivity can be assessed.

Terminology. Some of the complex isomers prepared in this study cannot be adequately distinguished within the framework of the existing recommended nomenclature system.[11] Therefore, a simple formalism allowing unambiguous characterization of the relevant isomers within the context of this study is now introduced, Figure 1.

If one coordinated amine group in Λ-[Co(en)$_2$(maleato)]$^+$ (**1**) reacts with the carbon–carbon double bond of the chelated maleate ligand in an intramolecular addition reaction, the amino acidate ligand *N*-(2-aminoethyl)aspartate (abbreviated: aea) is formed. Depending on which of the two carbon atoms C(A) or C(B) is attacked, two different isomers, **2** or **3**, result. One way of describing these isomers is by reference to the geometrical arrangement of the fused five-membered chelate rings of the co-

(1) Chemistry Department, Royal Veterinary and Agricultural University, Thorvaldsensvej 40, DK-1871 Copenhagen V, Denmark.
(2) C.S.I.R.O. Division of Environmental Mechanics, G.P.O. Box 821, Canberra, A.C.T. 2601, Australia.
(3) Metzler, D. E. "Biochemistry"; Academic Press: New York, 1977.
(4) Kurtz, D. M.; Holm, R. H.; Ruzicka, F. J.; Beinert, H.; Coles, C. J.; Singer, T. P. *J. Biol. Chem.* **1979**, *254*, 4967-4969.
(5) Glusker, J. P. *Acc. Chem. Res.* **1980**, *13*, 345-352 and references therein.
(6) Villafranca, J. J.; Mildvan, A. S. *J. Biol. Chem.* **1971**, *246*, 5791-5798 and references therein.
(7) Glusker, J. P. *J. Mol. Biol.* **1968**, *38*, 149-162.
(8) Patai, S.; Rappoport, Z. In "The Chemistry of Alkenes"; Patai, S., Ed.; Interscience: New York, 1964; Chapter 8.
(9) Burroughs Wellcome & Co. (U.S.A.) Inc. British Patent 901 455, 1962; *Chem. Abstr.* **1963**, *58*, 11374.
(10) Keat, Chong Eng Ph.D. Thesis, The Australian National University, 1979.
(11) IUPAC: "Nomenclature for Inorganic Chemistry", 2nd ed.; Butterworths: London, 1971; Section 7.5.

0002-7863/84/1506-2819$01.50/0

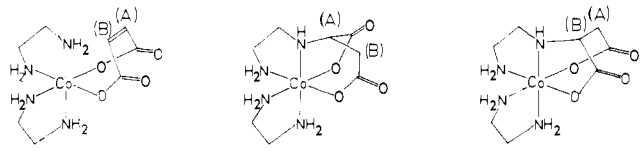

1 2 3

Figure 1. Λ-[Co(en)$_2$(maleato)]$^+$ (**1**), Λ-*fac*(5,5)-[Co(en)(*S*-aea)]$^+$ (**2**), and Λ-*mer*(5,5)-[Co(en)(*R*-aea)]$^+$ (**3**).

ordinated aea ligand. Isomer **2** is thus characterized by a facial arrangement of the tridentate unit $H_2N-CH_2-CH_2-NH-C(A)-H-COO^-$ and is denoted *fac*(5,5)-[Co(en)(aea)]$^+$. In **3** the corresponding tridentate unit, $H_2N-CH_2-CH_2-NH-C(B)H-COO^-$, is arranged in a meridional fashion, and the isomer is therefore denoted *mer*(5,5)-[Co(en)(aea)]$^+$.

The existing rules for the description of the absolute configuration of octahedral complexes relate only to tris- and bis-bidentate systems.[12] Additional or different rules are required in order to accommodate other types of octahedral chelate systems like those of isomers **2** and **3**. To simplify the ensuing discussion, the chiral isomers of *fac*(5,5)- and *mer*(5,5)-[Co(en)(aea)]$^+$ are assigned the absolute configuration of the parent chiral [Co(en)$_2$(maleato)]$^+$ complex (tris-bidentate) from which each isomer may be derived by an imagined intramolecular addition reaction occurring without change of the geometry around the metal center. Isomers **2** and **3** therefore both have the Λ absolute configuration.

For a given isomer, *fac*(5,5) or *mer*(5,5), of [Co(en)(aea)]$^+$ the chirality of the chiral carbon atoms of the aea ligand is, for steric reasons, linked to the absolute configuration of the relevant complex isomer, and vice versa. Thus in Λ-*fac*(5,5)-[Co(en)(*S*-aea)]$^+$ the chirality about C(A) is (*S*), and it is (*R*) in the Δ-isomer. Conversely, the chirality about C(B) in Λ-*mer*(5,5)-[Co(en)(*R*-aea)]$^+$ is (*R*), and it is (*S*) in the Δ-isomer.

Experimental Section

All chemicals were analytical grade. Commercial HO_3SCF_3 (3M Co.) was distilled before use. NaO_3SCF_3 was prepared from NaOH and HO_3SCF_3 in water followed by evaporation. AgO_3SCF_3 was synthesized from Ag_2O and HO_3SCF_3 in methanol. Commercial $NaPF_6$ (Ozark-Mahoning) was recrystallized before use. Liquid ammonia was used without further purification in containers open to the atmosphere. The amine $D_2NCH_2CH_2OD$ was obtained from ethanolamine by isotopic exchange in acidic D_2O (99.75%). Ethanolamine (30 mL) was mixed with D_2O (45 mL) and HO_3SCF_3 (0.10 g). The diluted D_2O was distilled at 16 torr (35–40 °C). Another batch of D_2O (15 mL) was added, and the exchanged D_2O/DHO was distilled off. This process was repeated twice and the deuterated amine finally collected by vacuum distillation (63–64 °C, 3.7 torr): ^{1}H NMR ($CDCl_3$) δ 2.8 (t, 2), 3.6 (t, 2).

Absorption and circular dichroism (CD) spectra were recorded with a Cary 14 spectrophotometer and a JASCO Model ORD/UV-5 instrument fitted with a Sproul Scientific SS 20 CD modification, respectively. The calibration standard for CD measurements was 2[(+)$_{589}$-[Co(en)$_3$]Cl$_3$]·NaCl·6H$_2$O (0.5 mM, in H_2O, $(\epsilon_l - \epsilon_r)_{490}^{max}$ +1.80 M^{-1} cm^{-1} per Co). All listed values of molar absorptivity (ε) and circular dichroism ($\Delta\epsilon = \epsilon_l - \epsilon_r$) are in units of M^{-1} cm^{-1}; water was used as the solvent unless otherwise specified. Optical rotations and rotatory dispersion (RD) spectra were monitored with a Perkin-Elmer P22 spectropolarimeter (±0.002°) in 1-dm quartz cells. Water was used as the solvent and the concentrations were 0.1% (w/v) unless otherwise specified. All listed values of specific rotations ($[\alpha]_\lambda$) are at 25.0 ± 0.1 °C in units of deg mL g^{-1} dm^{-1}. NMR spectra were recorded with JEOL 100-MHz Minimar (^{1}H) and JNM-FX 60 Fourier Transform (^{13}C) spectrometers at 30 and 25 °C, respectively, using sodium 3-(trimethylsilyl)propanesulfonate (TPS) in D_2O as an internal standard for ^{1}H spectra and 1,4-dioxane in D_2O for ^{13}C spectra. Chemical shifts δ, positive downfield, are given relative to these standards. The ion exchange resins AG 50W-X2 (cation) and Dowex 1-X8 (anion) were both 200–400 mesh (Bio-Rad). The SP-Sephadex C-25 cation exchange resin was purchased from Pharmacia. Dimensions of resin columns are given as diameter × length. Routinely, evaporation of solvents was carried out at reduced pressure (~20 torr) in a Büchi rotary evaporator using a water aspirator and water bath (40 °C). In order to avoid or limit decomposition, solvents used for recrystallizations were always preheated to the required maximum temperature before the compound to be recrystallized was added. The kinetics were followed by spectrophotometry using a Cary 118C spectrophotometer. A rapid mixing device was used for measurements of reaction rates down to $t_{1/2}$ ~1 s. This consisted of a small, hand-operated Teflon stopped-flow mixer, which introduced the solutions into a Helma quartz flow-through cell (1.00 cm) via two Teflon syringes (delivery volume 5 mL each). Both syringes could be filled independently, and the reservoirs, syringes, cell, and mixing chamber were maintained at 25.0 ± 0.1 °C. A Varian Techtron Model 1000 atomic absorption spectrophotometer was used for Co analyses of solutions. Elemental analyses of solid samples were performed by the Australian National University Analytical Services Unit. (**Caution**: Perchlorate salts are potentially hazardous and should not be heated).

[Co(en)$_2$(maleato)]ClO$_4$·0.5H$_2$O. A modification of a published method[13] was employed. Maleic acid (18 g) and [Co(en)$_2$CO$_3$]Br[14] (50 g) were ground together and added in portions to vigorously boiling water (1 L). The solution was boiled for 5 min, then cooled rapidly to 40 °C followed by concentration to 100 mL. The resulting viscous concentrate was kept at 4 °C overnight to allow carmine-colored crystals to separate. These were collected, washed with methanol–water (2:1, v/v) and methanol, and dried (10.7 g). Anal. Calcd for $CoC_8H_{18}N_4O_4Br·H_2O$: Co, 15.07; C, 24.57; H, 5.15; N, 14.33; Br, 20.43. Found: Co, 15.1; C, 24.7; H, 5.2; N, 14.5; Br, 21.5. The perchlorate salt was obtained by metathesis of the bromide salt (12 g) with $NaClO_4·H_2O$ (17 g) in boiling water (50 mL) followed by cooling to 0 °C. The separated crystalline product (9.9 g) was recrystallized from boiling water (50 mL) to yield large red crystals (7.7 g), which were collected and washed with methanol. Anal. Calcd for $CoC_8H_{18}N_4O_8Cl·0.5H_2O$: C, 14.67; C, 23.93; H, 4.77; N, 13.95. Found: Co, 14.5; C, 24.1; H, 4.8; N, 13.8. The N-deuterated complex salt [Co($D_2NCH_2CH_2ND_2$)$_2$(maleato)]ClO_4·0.5D_2O was obtained upon recrystallization of [Co(en)$_2$(maleato)]ClO_4·0.5H_2O (5.0 g) from D_2O (50 mL) with pD ~8 with use of triethanolamine (0.15 g) and 2 M DO_3SCF_3 (0.2 mL). The ^{1}H NMR spectrum of the product in 0.02 M DO_3SCF_3 showed no detectable resonances ascribable to N–H protons.

(+)$_{589}$-Λ- and (−)$_{589}$-Δ-[Co(en)$_2$(maleato)]ClO$_4$·1.5H$_2$O. Racemic [Co(en)$_2$(maleato)]Br·H_2O (23.5 g) in water (1 L) was passed through a column of Dowex 1-X8 anion exchange resin (4.5 × 12 cm) in the acetate form. The eluate of complex acetate salt was concentrated to 100 mL and (+)$_{589}$-Na_2[Sb_2((+)$_{589}$-tartrato)$_2$]·2H_2O (12.3 g) added. Crystals rapidly deposited, and after standing for 6 h the mixture was cooled in ice for 1 h. The carmine crystals (16.4 g) were collected, washed with methanol, and recrystallized from preheated boiling water (70 mL) (14.6 g). The specific rotations remained unchanged after recrystallization: $[\alpha]_{589}$ +264; $[\alpha]_{568}$ +303; $[\alpha]_{450}$ −387. Anal. Calcd for $CoC_{12}H_{22}H_4O_{11}Sb·4H_2O$: Co, 9.05; C, 22.14; H, 4.64; N, 8.61; Sb, 18.70. Found: Co, 9.0; C, 22.3; H, 4.7; N, 8.6; Sb, 18.4. The perchlorate salt was obtained by dissolving the product (14.6 g) in hot water (120 mL) and adding $NaClO_4·H_2O$ (21 g). After initial cooling to room temperature, the mixture was cooled in ice for 1 h and the deposited crystals were isolated by filtration, washed with methanol, and dried in the air (6.0 g). The specific rotations remained unchanged after recrystallization: $[\alpha]_{589}$ +316; $[\alpha]_{568}$ +376; $[\alpha]_{450}$ −813. Anal. Calcd for $CoC_8H_{18}N_4O_8Cl·1.5H_2O$: Co, 14.04;, C, 22.90; H, 5.04;, N, 13.55; Cl, 8.45. Found for ((+)$_{589}$-Λ-isomer): Co, 13.8; C, 23.0; H, 5.2; N, 13.2; Cl, 8.6. Visible spectrum (λ_{max}, ϵ_{max}): 499 nm, 124; 364 nm, 99. CD (λ_{max}, $\Delta\epsilon_{max}$): 528 nm, +0.91; 341 nm, +0.17.

The (−)$_{589}$-Λ-catoptric form was precipitated by adding $NaClO_4·H_2O$ (8.4 g) to the concentrated (50 mL) mother liquor from the initial crystallization of (+)$_{589}$-Λ-[Co(en)$_2$(maleato)]$_2$[Sb_2((+)$_{589}$-tartrato)$_2$]·8H_2O. After cooling in ice for 1 h the deposited crystals were collected and recrystallized twice from 60-mL portions of preheated boiling water yielding large carmine crystals (5.5 g). The specific rotations remained unchanged after recrystallization: $[\alpha]_{589}$ − 318; $[\alpha]_{568}$ − 378; $[\alpha]_{450}$ + 813. Anal. Found for ((−)$_{589}$-Δ-isomer): Co, 13.9; C, 23.6; H, 4.6; N, 13.6.

(+)$_{589}$-Λ-[Co(en)$_2$(maleato)]PF$_6$·2H$_2$O. (+)$_{589}$-Λ-[Co(en)$_2$(maleato)]ClO_4·1.5H_2O (0.8 g) was dissolved in hot water (15 mL, 80 °C) containing $NaPF_6$ (2.4 g). After the mixture was cooled to 0 °C the deposited pink crystals were collected and recrystallized from a solution of $NaPF_6$ (0.4 g) in water (15 mL). The product of fine needles was washed with ice-cold water and methanol and dried in the air (0.7 g). Anal. Calcd for $CoC_8H_{18}N_4O_4PF_6·2H_2O$: Co, 12.43; C, 20.26; H, 4.68; N, 11.82; P, 6.53. Found: Co, 12.2; C, 20.7; H, 4.3; N, 11.9; P, 6.4. Specific rotations: $[\alpha]_{589}$ + 283; $[\alpha]_{568}$ +336; $[\alpha]_{450}$ −728. Single crystals for X-ray crystallographic structure determination were grown by spon-

(12) Reference 11, Section 7.8.

(13) Duff, J. C. *J. Chem. Soc.* **1921**, *119*, 385–390.

(14) Springborg, J.; Schäffer, C. E. *Inorg. Synth.* **1973**, *14*, 63–77.

taneous evaporation of an aqueous solution at room temperature.

[Co(en)$_2$(maleato)]NO$_3$. Silver nitrate (1.7 g, 10 mmol) was added to a stirred solution of [Co(en)$_2$(maleato)]Br (3.9 g, 10 mmol) in water (10 mL). After filtration, the combined filtrate and washings were evaporated to 10 mL, and methanol (10 mL) was gradually added to crystallize a finely divided product (1.8 g). This was collected, washed thoroughly with methanol and ether, and dried in vacuo (0.1 torr) over P_4O_{10}. Anal. Calcd for $CoC_8H_{18}N_5O_7$: Co, 16.59; C, 27.05; H, 5.11; N, 19.72. Found: Co, 16.3; C, 26.8; H, 5.0; N, 19.4.

***mer*(5,5)-[Co(en)(aea)]ClO$_4$·0.5H$_2$O.** A solution of [Co(en)$_2$(maleato)]ClO$_4$·0.5H$_2$O (3.9 g) in liquid ammonia (100 mL) in a 1-L Büchi evaporation flask was swirled with $NaNH_2$ (0.2 g). After 2 min the reaction was quenched with NH_4Br (2.0 g) and the solvent evaporated completely at room temperature. The solid residue was suspended in aqueous 1 M $HClO_4$ (15 mL) and the undissolved orange material (2.5 g) collected and washed with ethanol. The solid product was recrystallized by dissolution in preheated boiling water (25 mL) followed by addition of $NaClO_4·H_2O$ (1.0 g) and ethanol (5 mL) and cooling to 0 °C. The fine, feathery, pink crystals were collected, washed with ethanol and ether, and dried in the air (1.9 g). Anal. Calcd for $CoC_8H_{18}N_4O_8Cl·0.5H_2O$: Co, 14.67; C, 23.92; H, 4.77; N, 13.95. Found: Co, 14.5; C, 24.1; H, 4.6; N, 13.9.

The N-deuterated complex *mer*(5,5)-[Co($D_2NCH_2CH_2ND_2$)(OOCCH($NDCH_2CH_2ND_2$)CH_2COO)]ClO$_4$ was obtained from the nondeuterated complex (1.6 g) by repeating the recrystallization and isolation procedure just described but using D_2O (20 mL) made to pD ~8 (with triethanolamine (0.15 g) and HO_3SCF_3 (0.040 g) as the recrystallization medium (yield: 1.4 g). The ^{1}H NMR spectrum of the product in Me_2SO-d_6 showed no detectable resonances ascribable to N–H protons.

An alternative procedure involved Me_2SO for the reaction medium. To a solution of [Co(en)$_2$(maleato)]ClO$_4$·0.5H$_2$O (7.8 g) in dry Me_2SO (30 mL) was added ethanolamine (5 mL). The solution was stirred for 30 min and poured slowly into a vigorously stirred mixture of anhydrous ether and absolute ethanol (9:1, v/v; 1 L). The stirred heterogeneous system was left until the solid material had transformed into fine orange-colored particles. These were collected and washed with ether. The deliquescent product was dissolved in hot water (50 mL), and after filtration of the hot solution, ethanol (20 mL) was added. On standing, fine orange-colored needles separated and further recrystallization was aided by cooling to 0 °C. The product (4.0 g) was recrystallized by dissolution in hot water (50 mL) followed by addition of $NaClO_4·H_2O$ (2.0 g) and ethanol (10 mL) and subsequent slow cooling to 0 °C. The separated crystals (3.2 g) were washed with ethanol and ether and dried in the air.

(−)$_{589}$-*mer*(5,5)-[Co(en)(aea)]ClO$_4$·0.5H$_2$O. To a solution of *mer*-(5,5)-[Co(en)(aea)]ClO$_4$·0.5H$_2$O (6.0 g, 15 mmol) in hot (80 °C) water (100 mL) was added Na_2(+)$_{589}$-tartrate·2H$_2$O (0.92 g, 4 mmol) and (+)$_{589}$-tartaric acid (0.63 g, 4 mmol). The resulting solution was left at room temperature overnight to deposit shiny crystalline rods (4.0 g), which were recrystallized from preheated, boiling water (160 mL) followed by cooling to 0 °C. The red crystals were washed with methanol and ether and dried in the air (1.5 g). The specific rotations remained unchanged after recrystallization: $[\alpha]_{589}$ −111; $[\alpha]_{520}$ +121. Anal. Calcd for $CoC_{12}H_{23}N_4O_{10}$: Co, 13.32; C, 32.58; H, 5.24; N, 12.67. Found: Co, 13.2; C, 33.6; H, 5.6; N, 12.7. The diastereoisomer (−)$_{589}$-*mer*(5,5)-[Co(en)(aea)](+)$_{589}$-(H)tartrate (0.44 g, 1.0 mmol) was treated at 0 °C with an ice-cold mixture of aqueous 70% $HClO_4$ (2.0 mL) and water (0.5 mL). After dissolution, ice-cold ethanol (10 mL) was cautiously added to precipitate fine red needles (0.47 g) of the perchlorate hydroxonium perchlorate double salt. (**Caution**: This mixture could be potentially explosive and should be kept cold at all times.) The collected crystals were recrystallized from a mixture of water (3 mL), ethanol (1 mL), and $NaClO_4·H_2O$ (0.1 g) affording large red bricks of the perchlorate salt. After cooling to 0 °C the crystals (0.27 g) were collected, washed with ethanol and ether, and dried in air. Anal. Calcd for $CoC_8H_{18}N_4O_8Cl·0.5H_2O$: Co, 14.67; C, 23.92; H, 4.77; N, 13.95. Found: Co, 14.6; C, 24.1; H, 4.6; N, 13.8. Visible spectrum (λ_{max}, ϵ_{max}): 479 nm, 139; 357 nm, 111. Specific rotations: $[\alpha]_{589}$ −135; $[\alpha]_{520}$ +118; $[\alpha]_{395}$ −51; $[\alpha]_{325}$ +257. CD (λ_{max}, $\Delta\epsilon_{max}$): 547 nm, −0.25; 473 nm, −0.037; 429 nm, +0.029; 348 nm, +0.031; 359 nm, −0.024; 332 nm, +0.080.

***mer*(5,5)-[Co(en)(aea)]NO$_3$.** Dissolved *mer*(5,5)-[Co(en)(aea)]ClO$_4$ was passed through a column of the NO_3^- form of Dowex 1-X8 anion exchange resin. The eluate of complex nitrate salt was concentrated until crystal formation commenced in the flask. Precipitation was completed by addition of ethanol and the solid product collected, washed with ethanol and ether, and dried in vacuo (0.1 torr) over P_4O_{10}. Anal. Calcd for $CoC_8H_{18}N_5O_7$: Co, 16.59; C, 27.05; H, 5.11; N, 19.72. Found: Co, 16.8; C, 27.0; H, 5.1; N, 19.9.

***mer*(5,5)-[Co(en)(aea)]O$_3$SCF$_3$.** A solution of *mer*(5,5)-[Co(en)(aea)]ClO$_4$ (1.0 g) in water (100 mL) was passed through a column of Dowex 1-X8 anion exchange resin (3 × 11 cm) in the Cl^- form and the total eluate concentrated to 15 mL. Glass beads and AgO_3SCF_3 (0.65 g) were added to the concentrate, and the resulting mixture was stirred until precipitation was complete. After filtration the filtrate was concentrated to 1 mL. Addition of excess ethanol precipitated a solid product (1.0 g), which was collected and recrystallized from a solution of NaO_3SCF_3 (0.25 g) in a mixture of water (6 mL) and ethanol (6 mL). The shiny orange-colored platelets (0.8 g) were collected, washed with ethanol and ether, and dried in vacuo (0.1 torr) over P_4O_{10}. Anal. Calcd for $CoC_9H_{18}F_3N_4O_7S$: Co, 13.33; C, 24.44; H, 4.10; N, 12.67; S, 7.25. Found: Co, 13.1; C, 24.4; H, 4.0; N, 12.6; S, 7.2.

***mer*(5,5)-[Co(en)(OOCCH(NHCH$_2$CH$_2$NH$_2$)CDHCOO)]O$_3$SCF$_3$.** A scaled-down version of the synthesis of *mer*(5,5)-[Co(en)(aea)]ClO$_4$ in Me_2SO was carried out. The N-deuterated complex [Co($D_2NCH_2CH_2ND_2$)$_2$(maleato)]ClO$_4$·0.5D$_2$O (1.95 g) was treated with $D_2NCH_2CH_2OD$ (1 mL) in Me_2SO (10 mL) for 30 min. The product perchlorate salt was isolated and recrystallized as described yielding 0.50 g of compound. This was converted to the $F_3CSO_3^-$ salt by the procedure already described yielding *mer*(5,5)-[Co(en)(OOCH(NHCH$_2$CH$_2$NH$_2$)CDHCOO)]O$_3$SCF$_3$ (0.35 g). ^{13}C NMR (D_2O): δ 118.0, 109.5, −7.3, −20.2, −21.2, −23.6, all singlets, −33.6 (t, J = 20 Hz). The entire procedure was repeated with *mer*(5,5)-[Co($D_2NCH_2CH_2ND_2$)(OOCCH($NDCH_2CH_2ND_2$)CH_2COO)]ClO$_4$·0.5D$_2$O (1.95 g). The experiment yielded *mer*(5,5)-[Co(en)(aea)]O$_3$SCF$_3$ with a ^{13}C NMR spectrum identical with that of the unlabeled complex.

***mer*(5,5)-[Co(en)(aea)(H$_2$O)]ClO$_4$·2H$_2$O.** Racemic *mer*(5,5)-[Co(en)(aea)]ClO$_4$·0.5H$_2$O (1.2 g) was dissolved in 2 M NaOH (3.0 mL) and rapidly filtered, and the filter was washed with water (1 mL). The filtrate was immediately acidified with glacial acetic acid (0.4 g) resulting in deposition of orance-colored crystals (1.0 g). These were recrystallized by dissolution in 1 M NaOH (4.5 mL) rapidly followed by filtration and addition of glacial acetic acid to the filtrate. The deposited orange-colored needles were collected, washed with methanol and ether, and dried in the air (0.76 g). Anal. Calcd for $CoC_8H_{20}N_4O_9Cl·2H_2O$: Co, 13.19; C, 21.51; H, 5.42; N, 12.54; Cl, 7.94. Found: Co, 13.3; C, 21.6; H, 5.4; N, 12.4; Cl, 7.9. Crystals for the X-ray crystallographic structure determination were grown from a dilute aqueous acetate–buffer solution (pH 4) by evaporation at room temperature.

(−)$_{589}$-Δ- and (+)$_{589}$-Λ-*fac*(5,5)-[Co(en)(aea)]Br. A solution of 2-(methoxycarbonylmethyl)-3-piperazinone[9] (34 g) and NaOH (16 g) in water (0.4 L) was heated on a steam bath for 20 min and subsequently diluted to 2 L with water. To the solution was added 1,2-ethanediamine (12 g) followed by aqueous HBr (48%, 34 g), $CoBr_2·6H_2O$ (65 g), and activated charcoal (5 g, "NORIT A"), and the mixture was aerated for 15 h. After filtration the solution was concentrated to 200 mL when crystallization commenced. The mixture was heated until all the crystals had redissolved, and ethanol (150 mL) was then aded with stirring to the hot solution from which orange-colored crystals soon deposited. After standing for 3 h the mixture was cooled in ice for 1 h. The collected crystalline product was washed with ethanol and ether and dried in the air (61 g). This product was contaminated with traces of [Co(en)$_3$]Br$_3$ (≤ 1%), which were removed by ion exchange chromatography. Anal. Calcd for $CoC_8H_{18}N_4O_4Br·H_2O$: Co, 15.07; C, 24.57; H, 5.15; N, 14.33. Found: Co, 14.7; C, 24.3; H, 5.2; N, 14.2.

The solution of racemic *fac*(5,5)-[Co(en)(aea)]Br·H$_2$O (43 g) in water (1.5 L) was passed down a column of Dowex 1-X8 anion exchange resin (4.5 × 30 cm) in the acetate form. The eluate of dissolved complex acetate salt was concentrated to 100 mL and treated with ammonium (+)$_{589}$-α-bromocamphorsulfonate, "NH_4BCS" (18 g). On standing overnight, orange-red crystals deposited (30 g). These were recrystallized from boiling water (100 mL) to yield large crystals, which were washed with ice-cold methanol and dried in the air (15.5 g). Further recrystallization left the specific rotations unaltered: $[\alpha]_{589}$ −74; $[\alpha]_{535}$ −184; $[\alpha]_{325}$ +1200. Anal. Calcd for $CoC_{18}H_{32}BrN_4O_8S·3H_2O$: Co, 8.96; C, 32.89; H, 5.83; Br, 12.15; N, 8.52; S, 4.88. Found: Co, 8.9; C, 33.0; H, 5.8; Br, 12.3; N, 8.2; S, 4.7. The perchlorate salt was obtained by dissolving the diastereoisomer (15.5 g) in a solution of aqueous 70% $HClO_4$ (17 g) in 1:1 (v/v) water–methanol (75 mL). On standing crystalline needles separated. These were collected, washed with methanol, and dried in vacuo (15 torr) over P_4O_{10} (6.7 g). Repeated crystallization did not change the specific rotations: $[\alpha]_{589}$ −195; $[\alpha]_{535}$ −406; $[\alpha]_{325}$ +276. Anal. Calcd for $CoC_8H_{18}N_4O_8Cl$: Co, 15.01; C, 24.47; H, 4.62; N, 14.27; Cl, 9.03. Found for ((−)$_{589}$-Δ): Co, 14.9; C, 24.4; H, 4.8; N, 14.1; Cl, 9.2.

The (+)$_{589}$-Λ-enantiomer was isolated by addition of $NaClO_4·H_2O$ (21 g) to the concentrated mother liquor (40 mL) from the initial crystallization of the (−)$_{589}$-Δ-*fac*(5,5)-[Co(en)(*R*-aea)]BCS diastereoisomer.

The separated crystals (9.9 g) were recrystallized from hot (80 °C) water (27 mL) yielding, after cooling to 0 °C, orange-red needles (3.9 g), which were collected, washed with methanol, and dried as above. Specific rotations: $[\alpha]_{589}$ +196; $[\alpha]_{535}$ +409; $[\alpha]_{325}$ −279. Found for ((+)$_{589}$-Λ): Co, 14.3; C, 24.9; H, 4.8; N, 14.3. Visible spectrum (λ_{max}, ϵ_{max}): 482 nm, 129; 358 nm, 104. CD (λ_{max}, $\Delta\epsilon_{max}$): 501 nm, +0.63; 373 nm, +0.42.

(+)$_{589}$-(*R*)- and (−)$_{589}$-(*S*)-*N*-(2-Aminoethyl)aspartic Acid. The (*R*)-amino acid was produced by decomposing (−)$_{589}$-Δ-*fac*(5,5)-[Co(en)(*R*-aea)]ClO_4 with H_2S. The complex (7.0 g) was dissolved in water (150 mL) and treated with H_2S. After filtration the solution was sorbed on a column (4.5 × 10 cm) of H^+ form AG 50W-X2 resin. The column was washed with water (50 mL) and eluted with aqueous ammoia (3.5 M). The eluate was reduced to an oil, which crystallized on trituration with a glass rod under methanol (50 mL). The collected product was recrystallized from water (40 mL) by slow addition of ethanol (40 mL). It was washed with ethanol and dried in vacuo (15 torr) over P_4O_{10} (2.3 g). Anal. Calcd for $C_6H_{12}N_2O_4$: C, 40.91; H, 6.87; N, 15.90. Found: C, 40.8; H, 7.1; N, 15.8. Specific rotation (1.0% in H_2O): $[\alpha]_{589}$ +29.4.

In the same manner (*S*)-*N*-(2-aminoethyl)aspartic acid was obtained from (+)$_{589}$-Λ-*fac*(5,5)-[Co(en)(*S*-aea)]ClO_4 in the same yield. Specific rotation (1.0% in H_2O): $[\alpha]_{589}$ −29.6.

***fac*(5,5)-[Co(en)(aea)]NO_3.** A solution of *fac*(5,5)-[Co(en)(aea)]Br (1.9 g) in water (200 mL) was sorbed on a column of H^+ form AG 50W-X2 cation exchange resin (2.5 × 1 cm). The column was washed with water (100 mL) and the orange-colored complex eluted with 1.5 M HNO_3 leaving a narrow yellow band ($[Co(en)_3]^{3+}$) on the column. The orange-colored eluate was neutralized with Na_2CO_3 and then concentrated to ~3 mL. Addition of excess ethanol precipitated a heterogeneous mixture of $NaNO_3$ and the complex nitrate salt, which was collected and recrystallized from a mixture of water (5 mL) and ethanol (5 mL). The collected product was extracted three times with 100-mL portions of boiling methanol and dried in vacuo (0.1 torr) over P_4O_{10}. Anal. Calcd for $CoC_8H_{18}N_5O_7$: Co, 16.59; C, 27.05; h, 5.11; N, 19.72. Found: Co, 16.5; C, 26.5; H, 5.5; N, 19.2.

Kinetic Studies. All reactions were followed spectrophotometrically in 1.00 M Na(ClO_4,OH) at 25.0 ± 0.05 °C. The reaction of *mer*-(5,5)-[Co(en)(aea)]ClO_4 (1.0 mM) with excess OH^- was monitored at 510, 460, and 400 nm. The reactions of [Co(en)$_2$(maleato)]ClO_4 (1.0 mM) or *fac*(5,5)-[Co(en)(aea)]Br (3.5 mM) with excess NaOH were followed at 495 and 410 nm, respectively. Mixing was performed with the rapid hand mixer described earlier. Solutions of NaOH were freshly prepared from May and Baker "Volucon" reagents with use of distilled CO_2-free water.

Product Distribution Analyses: [Co(en)$_2$(maleato)]$^+$ + OH^-. In a typical quantitative experiment NaOH (2 mL, 2.5 M) was rapidly added to a vigorously stirring solution of [Co(en)$_2$(maleato)]ClO_4·0.5H_2O (0.20 g) in water (8.0 mL) at 25 °C. After ~3 s the reaction solution was swiftly quenched with glacial acetic acid (0.6 g), diluted (~20 times) with water, and sorbed on a column of Na^+ form SP-Sephadex C-25 cation exchange resin (4 × 24 cm). The column was washed with 0.02 M CH_3COOH (300 mL) and the complex species eluted with 0.10 M citrate buffer solution, pH 3.8. Five bands separated, and the total eluate of each band was collected for Co analysis by atomic absorption spectorscopy. The bands were numbered in order of elution. An almost identical experiment quenched after 30 s was also performed. Two analogous experiments were carried out with the sample of complex initially dissolved in 18 mL of water and with reaction times of 6 and 60 s, respectively. Two experiments, each with reaction times of 120 min, were conducted in 0.50 M phosphate buffer pH 11.5, μ = 2.17 M (25 mL), and 0.25 M phosphate buffer pH 11.5, μ = 2.17 M ($NaClO_4$) (50 mL), respectively.

The same experiment was carried out with (+)$_{589}$-[Co(en)$_2$(maleato)]ClO_4·1.5H_2O (0.2 g) and quenched after 6 s. The rotary dispersion and visible absorption spectra of the eluates of bands 1, 2, 3, and 4 were recorded.

For further identification of the complexes constituting bands 1 and 3, a large-scale experiment was carried out. Aqueous NaOH (2 mL, 5 M) was added to a stirred solution of [Co(en)$_2$(maleato)]ClO_4·0.5H_2O (2 g) in water (48 mL) followed, after 60 s, by glacial acetic acid (1.2 g). The resulting solution was sorbed on a column (6 × 20 cm) of Na^+ form SP-Sephadex C-25 resin and elution carried out with 0.1 M citrate buffer, pH 3.8. Four clearly separated bands, corresponding to bands 1 (purple), 3 (red), 4 (orange), and 5 (pink) of the quantitative experiments above, appeared. The eluate of the purple band 1 was diluted (~4 times) with water and sorbed on a column (25 × 25 mm) of H^+ form AG 50W-X2 resin. After washing the column with 0.2 M HCl (200 mL), the complex was eluted with 3 M HCl and the eluate evaporated to dryness. The purple solid residue was dissolved in water (30 mL) and the complex decomposed by addition of Na_2S (0.1 g). After acidification with concentrated HCl (~0.5 mL) to expel excess S^{2-}, the mixture was filtered through "Supercel" (Hyflo) filteraid. The clear filtrate was passed down a column (25 × 25 mm) of H^+ form AG 50W-X2 resin in order to exchange all cationic species with H^+. The collected eluate was evaporated to dryness leaving a colorless solid residue. ^1H NMR (D_2O) δ 6.5 (s). The intensity of the singlet peak grew upon addition of authentic maleic acid with no extra peaks being observed. The procedure described above was repeated on band 3 to give the same end result.

[Co(en)$_2$(maleato)]ClO_4 with Base in Liquid NH_3 or Me_2SO. In a typical experiment (−)$_{589}$- or (+)$_{589}$-[Co(en)$_2$(maleato)]ClO_4·1.5H_2O (0.15 g) was dissolved in liquid NH_3 (~50 mL). Sodium amide (~0.02 g) was added to the stirred solution, and after 2 min the reaction mixture was neutralized with solid NH_4Br (0.2 g), which instantaneously changed the color of the solution from dark brown to orange. The solvent was removed completely in a rotary evaporator at room temperature. The resulting solid residue was suspended in a mixture of acetic acid (0.5 mL) and water (2.0 mL) and quantitatively transferred to the top of a column (24 × 240 mm) of AG 50W-X2 cation exchange resin, which had been prewashed with the eluant to be used. On elution with 0.5 M $NaClO_4$/0.05 M $HClO_4$ the complex species sorbed as a narrow band from which a red band (1) of unreacted starting material eluted first, followed by a major orange-colored band (2) of 1+ charge. A second orange-colored band (3) remained on the column and was finally eluted with 2 M HCl. The CD spectrum of the eluate from band 2 was recorded and the Co concentration of each eluate from all three bands was determined by atomic absorption spectroscopy.

Similar experiments were carried out in Me_2SO at 25 °C with use of $H_2NCH_2CH_2OH$ as the basic catalyst. A weighed sample (~0.15 g) of (+)$_{589}$- or (−)$_{589}$-[Co(en)$_2$(maleato)]ClO_4·1.5H_2O was dissolved in Me_2SO (3 mL) and ethanolamine (0.1 g) added to the stirring solution. After 15 min the solution was acidified with HO_3SCF_3 (0.7 g) in Me_2SO (3 mL) followed by dilution to 200 mL with water and sorption of the cations on a column (24 × 240 mm) of AG 50W-X2 cation exchange resin. Elution and analysis of eluates were performed as above to yield the same pattern.

Activated Charcoal Equilibrations of *fac*(5,5)- and *mer*(5,5)-[Co(en)(aea)]$^+$ and *mer*(5,5)-[Co(en)(aea)(H_2O)]$^+$. A solution of (−)$_{589}$-*fac*(5,5)-[Co(en)(aea)]ClO_4 (0.05 g) in water (40 mL) was mixed with activated charcoal powder (~0.05 g, "Norit A", Matheson, Coleman and Bell) and the heterogeneous mixture stirred in a water-jacketed glass vessel kept at 80 ± 1 °C. Filtered samples (~2 mL) of the reaction mixture were taken at regular intervals and the optical rotary dispersion of each sample monitored. When no further change in the optical activity was detectable (~1 h), the entire reaction mixture was filtered and sorbed on a column (25 × 60 mm) of AG 50W-X2 cation exchange resion. Elution with 0.5 M $NaClO_4$/0.05 M $HClO_4$ separated three bands. A leading, very minor (<2%, estimated), purple band (1) was followed by the orange-colored main band (2) of 1+ charge. On the column remained a minor (<2%, estimated) band (3) of higher charge. The eluate of band 2 was collected, the CD spectrum recorded, and the Co concentration determined by atomic absorption spectroscopy. An analogous experiment was carried out with (−)$_{589}$-*mer*(5,5)-[Co(en)(aea)]ClO_4·0.5H_2O as the starting material; a longer reaction time (~12 h) was required before equilibrium was attained.

A solution of (−)$_{589}$-*mer*(5,5)-[Co(en)(aea)](+)$_{589}$-(H)tartrate (~0.1 g) in 2 M NaOH (2 mL) was stirred for 35 min. The solution was neutralized to pH 6.5 with glacial acetic acid and diluted to ~40 mL with water and activated charcoal powder was added. The mixture was equilibrated at 80 ± 1 °C, and the products were separated and analyzed as described above for (−)$_{589}$-*fac*(5,5)-[Co(en)(aea)]ClO_4.

Reaction of *mer*(5,5)-[Co(en)(aea)]O_3SCF_3 with OD^- in D_2O. In a series of experiments with variable reaction times, NaOD (2.0 M, 1.0 mL) was swiftly added to a stirring solution of *mer*(5,5)-[Co(en)(aea)]O_3SCF_3 (0.20 g) in D_2O (4.0 mL), followed a specified number of seconds later by DO_3SCF_3 (2 M, 1.0 mL), and adjustment of pD to 1.5 with 1 M DO_3SCF_3. The volume was carefully reduced by evaporation to ~1.5 mL at room temperature, and the ^{13}C NMR spectrum of the solution was recorded without delay.

mer(5,5)-[Co(en)(aea)(H_2O)]ClO_4·2H_2O (0.6 g) was dissolved in D_2O (1.5 mL) by adjusting the pD of the solution to 1.5–2 with 4 M DCl. The ^{13}C NMR spectrum was recorded immediately after the addition.

X-ray Diffraction Studies of (+)$_{589}$-Λ-[Co(en)$_2$(maleato)]PF_6·2H_2O, *mer*(5,5)-[Co(en)(aea)(H_2O)]ClO_4·2H_2O, and (−)$_{589}$-Δ-*fac*(5,5)-[Co(en)(aea)]BCS·3H_2O. The relevant crystal data and details of the intensity measurements are summarized in Table I.

Clear, red crystals of Δ-*fac*(5,5)-[Co(en)(*R*-aea)]BCS·3H_2O and [Co(en)(aea)(H_2O)]ClO_4·2H_2O were mounted on the end of glass fibers while those of Λ-[Co(en)$_2$(maleato)]PF_6·2H_2O, also clear red, were sealed in 0.3-mm diameter Lindemann glass capillaries. Preliminary precession photographs of Δ-*fac*(5,5)-[Co(en)(*R*-aea)]BCS·3H_2O indicated the

Table I. Crystal Data

compound	Λ-[Co(en)$_2$(maleato)]PF$_6$·2H$_2$O	Δ-*fac*(5,5)-[Co(en)(aea)]BCS·3H$_2$O	[Co(en)(aea)(H$_2$O)]ClO$_4$·2H$_2$O
crystal system	monoclinic	triclinic	monoclinic
space group	$P2_1$	$P\bar{1}$	$P2_1/c$
a, Å	11.629 (6)	6.976 (1)	7.191 (1)
b, Å	7.701 (4)	7.242 (1)	10.915 (2)
c, Å	9.379 (4)	14.248 (2)	20.723 (6)
α, deg		76.89 (1)	
β, deg	97.18 (1)	84.61 (1)	91.41 (1)
γ, deg		70.86 (1)	
vol., Å^3	833.3	662.1	1626.1
mol. wt.	474.2	657.4	446.7
Z	2	1	4
ρ(calcd), g/cm^3	1.890	1.649	1.824
ρ(measd), g/cm^3	1.822	1.634	1.808
crystal size, mm^3	0.12 × 0.12 × 0.50	0.21 × 0.18 × 0.08	0.16 × 0.19 × 0.32
μ, cm^{-1}	12.76	24.14	13.32
no. of obsd refl	4336	4731	4796
no. of refl scanned (including standards)	5283	7458	8196

crystal system to be triclinic; the space group $P\bar{1}$ (C_i^1, No. 1)[15] was chosen on the basis of the optical activity of Δ-*fac*(5,5)-[Co(en)(*R*-aea)]-BCS·3H$_2$O. Precession and Weissenberg photographs of crystals of the other two compounds indicated the crystal system to be monoclinic with systematically absent reflections ($h0l$ for $l \neq 2n$ and $0k0$ for $k \neq 2n$) for [Co(en)(aea)(H$_2$O)]ClO$_4$·2H$_2$O uniquely determining its space group as $P2_{1/c}$ (C_{2h}^5, No. 14)[16] and with the optical activity and systematically absent reflections ($0k0$ for $k \neq 2n$) for Λ-[Co(en)$_2$(maleato)]PF$_6$·2H$_2$O determining its space group as $P2_1$ (C_2^2, No. 4).[17]

The lattice constants of all three compounds were determined by a least-squares analysis[18] of the 2θ, ω, and χ values for 12 carefully centered reflections ($2\theta > 27°$) measured with a Picker FACS-1 automatic diffractometer with (graphite) crystal monochromated Mo Kα radiation (λ 0.71069 Å). The observed densities were measured by flotation with use of a solution of carbon tetrachloride and 1,2-dibromoethane for Λ-[Co(en)$_2$(maleato)]PF$_6$·2H$_2$O and Δ-*fac*(5,5)-[Co(en)(*R*-aea)]BCS·3H$_2$O and a solution of chloroform and 1,2-dibromomethane for [Co(en)-(aea)(H$_2$O)]ClO$_4$·2H$_2$O.

The intensity data for all three compounds were measured on the Picker diffractometer with use of the $\theta - 2\theta$ scan technique with (graphite) crystal monochromated Mo Kα radiation at a take-off angle of ~3°. 2θ was varied from 3 to 70° for Λ-[Co(en)$_2$(maleato)]PF$_6$·2H$_2$O and [Co(en)(aea)(H$_2$O)]ClO$_4$·2H$_2$O and from 3 to 60° for Δ-*fac*-(5,5)-[Co(en)(*R*-aea)]BCS·3H$_2$O. The range of each scan, taken at 2°/min, consisted of the estimated base width of 1.60° at $2\theta = 0°$ and an increment of $\Delta(2\theta) = (0.692 \tan \theta)°$ to allow for spectral dispersion; backgrounds were recorded for 10-s duration at each extremity of the reflection scan (in stationary crystal-stationary counter mode) and were assumed to vary linearly across the scan. The intensities of three reference reflections, measured at 97-reflection intervals to monitor the stability of the system, displayed no trend with time for Λ-[Co(en)$_2$-(maleato)]PF$_6$·2H$_2$O. However, for Δ-*fac*(5,5)-[Co(en)(*R*-aea)]BCS·3H$_2$O and [Co(en)(aea)(H$_2$O)]ClO$_4$·2H$_2$O the intensities of the three reference reflections decreased linearly to values of 90% and 95%, respectively, of their original values. The intensity data were corrected accordingly.

The intensity data were reduced to values of $|F_o|$ and $\sigma(F_o)$ with use of algorithms described elsewhere.[19] Sample corrections for the effects of absorption were made for the intensity data of all three compounds. The transmission factors for Λ-[Co(en)$_2$(maleato)]PF$_6$·2H$_2$O and [Co-(en)(aea)(H$_2$O)]ClO$_4$·2H$_2$O varied from 0.92 to 0.94 and from 0.87 to 0.91, respectively; absorption corrections were therefore not made. For Δ-*fac*(5,5)-[Co(en)(*R*-aea)]BCS·3H$_2$O the transmission factors varied from 0.78 to 0.87 and the intensity data for that compound were corrected for absorption effects with use of the method of De Meulenaer and Tompa.[20] The uncertainty constant (p^2)[21] was set equal to 0.002. For all three compounds those reflections with $I > 3\sigma(I)$ were retained for use in subsequent structure analysis.

Structure Determination and Refinement. All three structures were solved by straightforward application of the heavy-atom method. A three-dimensional Patterson synthesis revealed the position of the Co atom for Λ-[Co(en)$_2$(maleato)]PF$_6$·2H$_2$O and [Co(en)(aea)(H$_2$O)]-ClO$_4$·2H$_2$O and the Co, Br, and S atoms for Δ-*fac*(5,5)-[Co(en)(*R*-aea)]BCS·3H$_2$O. The remainder of the non-hydrogen atoms (excluding the waters of crystallization) were located from subsequent Fourier syntheses. For Λ-[Co(en)$_2$(maleato)]PF$_6$·2H$_2$O, the PF$_6^-$ anion appeared to be disordered; the six largest peaks around the phosphorus atom that gave acceptable P–F bond lengths and reasonable octahedral geometry were chosen as fluorine atoms.

Atomic coordinates and isotropic thermal parameters were refined by a full-matrix least-squares analysis; a difference Fourier was then calculated to locate the solvent molecules and hydrogen atoms. One of the two waters of crystallization in [Co(en)(aea)(H$_2$O)]ClO$_4$·2H$_2$O was disordered. Site occupancies of 0.50 were assigned on the basis of relative peak heights and were not varied during subsequent least-squares calculations.

For Δ-*fac*(5,5)-[Co(en)(*R*-aea)]BCS·3H$_2$O all of the hydrogen atoms were located in the difference Fourier, while all but those of the waters of crystallization were located for [Co(en)(aea)(H$_2$O)]ClO$_4$·2H$_2$O. Positions of the hydrogen atoms of the complex cation in Λ-[Co(en)$_2$-(maleato)]PF$_6$·2H$_2$O were calculated with N–H = 1.00 Å and C–H = 1.05 Å. In all cases, the coordinates and isotropic thermal parameters (assigned a value slightly larger than the isotropic thermal parameter of the atom to which the hydrogen is bonded) of the hydrogen atoms were included in the subsequent least-squares calculations but were not varied.

Refinement of the scattering model, with anisotropic thermal parameters assigned to all non-hydrogen atoms, was continued by using a block-diagonal least-squares analysis. The correct absolute configuration of the complex cation in Λ-[Co(en)$_2$(maleato)]PF$_6$·2H$_2$O was determined by comparison of F_o and F_c for the Friedel pairs of 30 strong reflections and was confirmed by an increase in R_1 from 0.0463 to 0.0585 on changing the signs of the imaginary component of the anomalous dispersion. The absolute configuration of the Δ-*fac*(5,5)-[Co(en)(*R*-aea)]$^+$ cation was assigned by using the known configuration of the $(+)_{589}$-bromocamphorsulfonate anion and was confirmed as for Λ-[Co(en)$_2$-(maleato)]PF$_6$·2H$_2$O.

Upon convergence the R_1 and R_2 values were 0.045 and 0.060, respectively, for Λ-[Co(en)$_2$(maleato)]PF$_6$·2H$_2$O, 0.040 and 0.044, respectively, for Δ-*fac*(5,5)-[Co(en)(*R*-aea)]BCS·3H$_2$O, and 0.045 and 0.058, respectively, for [Co(en)(aea)(H$_2$O)]ClO$_4$·2H$_2$O, where:

$$R_1 = \frac{\sum||F_o| - |F_c||}{\sum|F_o|}$$

and

$$R_2 = \left[\frac{\sum w(|F_o| - |F_c|)^2}{\sum w|F_o|^2}\right]^{1/2} \qquad w = \frac{1}{\sigma^2(F_o)}$$

(15) "International Tables for X-Ray Crystallography", 3rd ed.; Henry, N. F. M., Lonsdale, K., Eds.; Kynoch Press: Birmingham, 1969; Vol. 1, p 74.
(16) Reference 15, p 99.
(17) Reference 15, p 79.
(18) The Picker Corporation FACS-1 Disk Operating System was used for all phases of diffractometer control.
(19) Robertson, G. B.; Whimp, P. O. *J. Am. Chem. Soc.* **1975**, *97*, 1051–1059.
(20) De Meulenaer, J.; Tampa, H. *Acta Crystallogr.* **1965**, *19*, 1014–1018.
(21) Busing, W. R.; Levy, H. A. *J. Chem. Phys.* **1957**, *26*, 563–568. Corfield, P. W. R.; Doedens, R. J.; Ibers, J. A. *Inorg. Chem.* **1967**, *6*, 197–204.

The quantity minimized during the least-squares refinement was $\sum w(|F_o| - |F_c|)^2$. For Λ-$[Co(en)_2(maleato)]PF_6 \cdot 2H_2O$ in the final cycle of refinement no parameter of an atom in the complex cation shifted by more than 0.10σ and no parameter of an atom of the PF_6^- anion by more than 0.34σ. The maximum shifts in parameters in the final cycle for Δ-*fac*-(5,5)-[Co(en)(*R*-aea)]BCS·$3H_2O$ and $[Co(en)(aea)(H_2O)]ClO_4 \cdot 2H_2O$ were 0.15 and 0.10σ, respectively.

A final difference Fourier synthesis for Λ-$[Co(en)_2(maleato)]PF_6 \cdot 2H_2O$ was essentially featureless with the six largest peaks (0.8–1.3 ē/Å^3) located near Co, Cl, O1, or the PF_6^- anion. For Δ-*fac*(5,5)-[Co(en)(*R*-aea)]BCS·$3H_2O$ a final difference Fourier synthesis revealed ten peaks in the range 0.7–1.0 ē/Å^3, all near Br, Co, or S. A final difference Fourier synthesis for $[Co(en)(aea)(H_2O)]ClO_4 \cdot 2H_2O$ was featureless except for a residual (1.4 ē/Å^3) near N3.

Atomic scattering factors and corrections for the real and imaginary parts of the anomalous dispersion were taken from ref 22. Calculations were performed on the UNIVAC 1100/42 computer of the Australian National University Computer Services Centre with use of programs of the ANUCRYS package.[19] The molecular drawings were produced by using an ANUCRYS implementation of ORTEP.[23]

Results

Synthesis. $[Co(en)_2(maleato)]^+$. The bromide salt was synthesized by adding an equimolar mixture of $[Co(en)_2(CO_3)]Br$ and maleic acid to a large volume of boiling water. Reducing the volume caused the product to crystallize. This rather simple procedure is similar to the method first published in 1921 by Duff.[13] The method, as applied here, reproducibly gave ~20% $[Co(en)_2(maleato)]Br \cdot H_2O$. The racemic complex was resolved by precipitation of the $(+)_{589}$-Λ-isomer with $[Sb_2((+)_{589}\text{-tartrato})_2]^{2-}$ as the less soluble diastereoisomer, and both catoptric forms were obtained as perchlorates optically pure.

The $[Co(en)_2(maleato)]^+$ ion was stable in neutral and dilute acid solutions at ambient temperature but was reactive with base and also lost the maleato ligand in strong HCl or HBr solutions. The acid-catalyzed hydrolysis is a characteristic of Co(III) carboxylato complexes.[24] The base-catalyzed path involves addition of deprotonated ethylenediamine to the olefinic bond to give a chelated aminoethylaspartic acid complex.

***mer*(5,5)-[Co(en)(aea)]$^+$** was obtained by allowing $[Co(en)_2(maleato)]ClO_4 \cdot 0.5H_2O$ to react with $NaNH_2$ in liquid ammonia, followed by quenching with excess NH_4Br. An alternative procedure utilized Me_2SO as the solvent and ethanolamine as the base catalyst. Both methods were equally reliable but the latter procedure was the more cumbersome of the two.

When $[Co(D_2NCH_2CH_2ND_2)_2(maleato)]ClO_4 \cdot 0.5D_2O$ (in which all labile proton positions were deuterated) was employed as the substrate in Me_2SO (with $D_2NCH_2CH_2OD$ as the base catalyst), one "nonlabile" D atom was incorporated on the β-carbon atom of the aspartate moiety in the product complex. This was ascertained from its ^{13}C NMR spectrum in which the resonance at δ −33.6, seen as a singlet in the nonlabeled compound, now appears as a doublet with a coupling constant (J = 20 Hz) typical for ^{13}C–D coupling. In the hydrogen nondecoupled spectrum of the nonlabeled complex, the same carbon resonance was seen as a triplet consistent with coupling of the carbon atom to two protons. Since it would seem chemically unreasonable that any of the methylene groups of the ethylenediamine moieties would have been deuterated during the addition reaction, all the evidence is consistent with deuteration on the β-carbon of the aspartate moiety of the generatred aea ligand. This deuterium incorporation must have occurred as part of the intramolecular addition reaction and could not have arisen from a subsequent exchange reaction since no such incorporation was seen when *mer*(5,5)-[Co(D$_2$NCH$_2$CH$_2$ND$_2$)(OOCCH(NDCH$_2$CH$_2$ND$_2$)CH$_2$COO)]ClO$_4$ was subjected to the above synthetic conditions for prolonged periods of time.

The two protons on the β-carbon of the aspartate moiety of aea are diastereotopic and the deuteration could have occurred stereospecifically. However, the ^1H NMR spectrum of *mer*-(5,5)-[Co(D$_2$NCH$_2$CH$_2$ND$_2$)(OOCCH(NDCH$_2$CH$_2$ND$_2$)-CDHCOO)]$^+$ was not consistent with this and indicated a 50:50 distribution of deuterium over the two diastereotopic sites.

Resolution of the racemic complex was accomplished by fractional recrystallization of the $(-)_{589}$-*mer*(5,5)-[Co(en)-(aea)]$(+)_{589}$-(H)tartrate diastereoisomer, which was finally converted to the ClO_4^- salt.

The *mer*(5,5)-[Co(en)(aea)]$^+$ ion was stable in neutral and dilute acid solutions but hydrolyzed rapidly in the presence of base (vide infra).

***mer*(5,5)-[Co(en)(aea)(H$_2$O)]$^+$.** Treatment of racemic *mer*-(5,5)-[Co(en)(aea)]$ClO_4 \cdot 0.5H_2O$ with strong aqueous base cleaved one of the carboxylate groups from the Co(III) ion, and addition of acetic acid to pH ~4 caused the perchlorate salt of the resulting aqua complex to crystallize. Isolation of the corresponding chiral complex by a similar procedure using $(-)_{589}$-*mer*(5,5)-[Co(en)-(aea)]$ClO_4 \cdot 0.5H_2O$ was not successful despite attempts to crystallize the product with a variety of anions.

Potentiometric titration of an equimolar mixture of *mer*-(5,5)-[Co(en)(aea)(H$_2$O)]$ClO_4 \cdot 2H_2O$ and $HClO_4$ in water with 1 M NaOH yielded a two-step titration curve consistent with the presence of two protic equilibria at pK_a 3.3 and 7.0 (25 °C, μ = 1.0 M ($NaClO_4$)). These are attributed to the free carboxylic acid and the coordinated H_2O, respectively. Back-titration with 1 M HCl yielded a slightly different result (~−0.3 pH units), but some decomposition of the complex at high pH was suspected to cause this discrepancy.

***fac*(5,5)-[Co(en)(aea)]$^+$.** The ligand *N*-(2-aminoethyl)aspartate was synthesized by way of the lactam monomethyl ester, 2-(methoxycarbonylmethyl)-3-piperazinone. An early patent[25] reports a similar method claiming to yield the *N*-(2-aminoethyl)aspartate dimethylester directly. Repetition of the patented procedure only produced the lactam monoester, which, however, was readily hydrolyzed in situ to give *N*-(2-aminoethyl)aspartate, aea. The Co complex was then synthesized from equimolar amounts of ethylenediamine, $CoBr_2 \cdot 6H_2O$, and aea via aerobic oxidation in the presence of activated charcoal. Significantly lower yields of the product and large proportions of $[Co(en)_3]Br_3$ byproduct arose if the oxidation process was not carried out in a relatively large reaction volume. At high bromide ion concentration,[5] precipitation of $[Co(en)_3]Br_3$ occurred. This complication was largely avoided by high dilution, but the isolated product of *fac*(5,5)-[Co(en)(aea)]Br·H_2O always contained a minor fraction of the $[Co(en)_3]Br_3$ impurity. Recrystallization was a relatively inefficient means of removing this impurity, but cation exchange chromatography, as described for the synthesis of the nitrate salt, efficiently separated the $[Co(en)_3]^{3+}$ ion from the *fac*(5,5)-[Co-(en)(aea)]$^+$ complex.

Resolution of the racemic complex was achieved by precipitating and recrystallizing the $(-)_{589}$-Δ-*fac*(5,5)-[Co(en)(*R*-aea)]$^+$ isomer as the $(+)_{589}$-α-bromocamphorsulfonate (BCS^-) salt, which was then converted to the perchlorate salt $(-)_{589}$-Δ-*fac*(5,5)-[Co-(en)(*R*-aea)]ClO_4. The catoptric form, $(+)_{589}$-Λ-*fac*(5,5)-[Co-(en)(*S*-aea)]ClO_4, was isolated from the mother liquor.

The chirality of the coordinated quadridentate aea ligand is inextricably linked to the absolute configuration of the metal complex for any one of the [Co(en)(aea)]$^+$ isomers (*fac*(5,5) or *mer*(5,5)). Hence, resolution of the ligand was achieved at the same time as resolution of the complex. (*R*)-*N*-(2-Aminoethyl)aspartic acid was produced from the $(-)_{589}$-Δ-*fac*(5,5)-[Co(en)(*R*-aea)]$^+$ ion and the (*S*)-amino acid from the $(+)_{589}$-Λ-*fac*(5,5) complex.

UV–visible, RD, and CD spectra are given in Figure 2.

Structural Studies. Aspects of the structures of the complexes Λ-$[Co(en)_2(maleato)]PF_6 \cdot 2H_2O$, Δ-*fac*(5,5)-[Co(en)(*R*-aea)]-BCS·$3H_2O$, and $[Co(en)(aea)(H_2O)]ClO_4 \cdot 2H_2O$ needed to be

(22) "International Tables for X-Ray Crystallography"; Ibers, J. A., Hamilton, W. C., Eds.; Kynoch Press: Birmingham, 1974; Vol. IV, pp 99–101, 149–150.

(23) Johnson, O. K., Report ORNL-3794, Oak Ridge National Laboratory, Oak Ridge, TN, 1965.

(24) Przystas, T. J.; Ward, J. R.; Haim, A. *Inorg. Chem.* **1973**, *12*, 743–749.

(25) Bersworth, F. C.; Frost, A. E. U.S. Patent 2761874, 1956; *Chem. Abstr.* **1957**, *51*, 3658i.

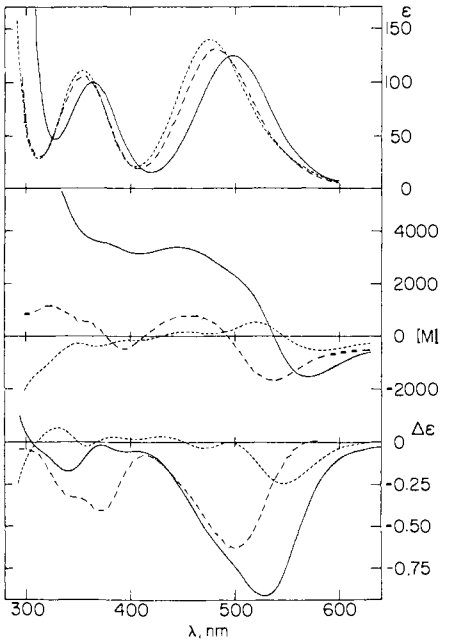

Figure 2. Absorption, rotatory dispersion, and circular dichroism spectra of $(+)_{589}$-[Co(en)$_2$(maleato)]$ClO_4 \cdot 1.5H_2O$ (—), $(-)_{589}$-*mer*-[Co(en)(aea)]$ClO_4 \cdot H_2O$ (---), and $(+)_{589}$-*fac*(5,5)-[Co(en)(aea)]ClO_4 (·--), all in water.

Table II. Final Atomic Fractional Coordinates for Λ-[Co(en)$_2$(maleato)]$PF_6 \cdot 2H_2O$[a]

atom	*x/A*	*y/B*	*z/C*
Co	0.2164 (1)	−0.5000	0.0237 (1)
O(1)	0.1399 (2)	−0.2840 (3)	0.0500 (3)
O(2)	0.3335 (2)	−0.4027 (3)	−0.0771 (3)
O(3)	0.1206 (2)	−0.0030 (4)	0.0594 (3)
O(4)	0.4853 (2)	−0.2540 (4)	−0.1228 (3)
O(5)	0.5419 (4)	0.0052 (6)	0.3682 (3)
O(6)	0.5197 (3)	−0.3523 (5)	0.3788 (4)
N(1)	0.0987 (3)	−0.6119 (4)	0.1195 (3)
N(2)	0.3102 (2)	−0.5013 (6)	0.2114 (3)
N(3)	0.2789 (2)	−0.7200 (4)	−0.0245 (3)
N(4)	0.1214 (2)	−0.5160 (5)	−0.1616 (3)
C(1)	0.1825 (3)	−0.1338 (4)	0.0750 (4)
C(2)	0.3062 (3)	−0.1052 (4)	0.1286 (4)
C(3)	0.3993 (3)	−0.1632 (5)	0.0739 (4)
C(4)	0.4053 (3)	−0.2792 (4)	−0.0496 (4)
C(5)	0.2590 (4)	−0.6223 (5)	0.3079 (4)
C(6)	0.1301 (4)	−0.6002 (6)	0.2768 (5)
C(7)	0.2567 (4)	−0.7449 (6)	−0.1804 (5)
C(8)	0.1349 (4)	−0.6898 (6)	−0.2256 (4)
P	0.1847 (1)	−0.1418 (2)	0.5329 (1)
F(1)	0.0874 (7)	−0.1331 (14)	0.4171 (11)
F(2)	0.1291 (6)	−0.0812 (11)	0.6616 (10)
F(3)	0.2917 (6)	−0.1475 (8)	0.6495 (6)
F(4)	0.2456 (7)	−0.2056 (8)	0.4122 (6)
F(5)	0.2310 (5)	0.0456 (5)	0.5076 (5)
F(6)	0.1476 (8)	−0.3294 (7)	0.5603 (5)

[a] The figure in parentheses following each datum is the estimated standard deviation in the last significant figure.

established with certainty, and X-ray crystallographic studies on the complexes were carried out. Their atomic coordinates are presented in Tables II–IV, respectively. Tables of anisotropic thermal parameters, tables of observed and calculated structure factor amplitudes, the results of least-squares mean planes calculations, and bond lengths and angles for the anions for all three compounds, as well as final atomic coordinates and isotropic thermal parameters for the hydrogen atoms of Δ-*fac*(5,5)-[Co(en)(*R*-aea)]$BCS \cdot 3H_2O$ and [Co(en)(aea)(H_2O)]$ClO_4 \cdot 2H_2O$, are available as Supplementary Material. The bond lengths and angles in the complex cations of all three compounds are given in Table V. Figure 3 shows perspective views of the three cobalt(III) complexes.

Table III. Final Atomic Fractional Coordinates for Δ-*fac*(5,5)-[Co(en)(aea)]$BCS \cdot 3H_2O$[a]

atom	*x/A*	*y/B*	*z/C*
Br	1.0	0.0	0.0
Co	0.9747 (1)	0.2454 (1)	0.5056 (1)
S	0.5656 (2)	0.7318 (2)	0.2111 (1)
O(1)	0.7243 (4)	0.1857 (5)	0.5261 (2)
O(2)	1.1223 (5)	−0.0337 (4)	0.5476 (2)
O(3)	0.5460 (5)	0.0550 (6)	0.6458 (2)
O(4)	1.2406 (6)	−0.3191 (5)	0.6493 (3)
O(5)	0.5856 (6)	0.2586 (7)	−0.1126 (3)
O(6)	0.3619 (6)	0.7395 (7)	0.2481 (3)
O(7)	0.7168 (6)	0.5552 (5)	0.2578 (2)
O(8)	0.6085 (6)	0.9132 (5)	0.2129 (2)
N(1)	0.8314 (5)	0.5282 (5)	0.4623 (2)
N(2)	0.9212 (5)	0.2928 (5)	0.6364 (2)
N(3)	1.2410 (6)	0.2813 (6)	0.4833 (3)
N(4)	0.9971 (5)	0.2039 (5)	0.3742 (2)
C(1)	0.6875 (7)	0.1239 (6)	0.6157 (3)
C(2)	0.8329 (7)	0.1347 (7)	0.6860 (3)
C(3)	1.0013 (9)	−0.0613 (7)	0.7141 (3)
C(4)	1.1305 (7)	−0.1431 (6)	0.6323 (3)
C(5)	0.7763 (8)	0.4998 (7)	0.6324 (3)
C(6)	0.8227 (8)	0.6322 (7)	0.5408 (4)
C(7)	1.3383 (8)	0.1978 (8)	0.3973 (4)
C(8)	1.1791 (8)	0.2485 (8)	0.3253 (3)
C(9)	0.7616 (7)	0.2041 (6)	0.0349 (3)
C(10)	0.7966 (6)	0.3597 (6)	0.0787 (3)
C(13)	0.5994 (7)	0.5391 (7)	−0.0497 (3)
C(14)	0.6394 (7)	0.3240 (8)	−0.0532 (3)
C(15)	0.5862 (6)	0.5256 (6)	0.0618 (3)
C(16)	0.5724 (6)	0.7252 (6)	0.0867 (3)
C(17)	0.4079 (7)	0.4590 (8)	0.1095 (4)
C(11)	0.9405 (7)	0.4526 (8)	0.0135 (4)
C(12)	0.8100 (9)	0.5710 (8)	−0.0763 (4)
C(18)	0.4240 (10)	0.6849 (10)	−0.1118 (4)
O(9)	0.9652 (6)	0.8409 (6)	0.3138 (2)
O(10)	0.2053 (6)	0.3269 (8)	0.7582 (3)
O(11)	0.3786 (5)	0.6343 (5)	0.4521 (2)

[a] The figure in parentheses following each datum is the estimated standard deviation in the last significant figure.

Table IV. Final Atomic Fractional Coordinates for [Co(en)(aea)(H_2O)]$ClO_4 \cdot 2H_2O$[a]

atom	*x/A*	*y/B*	*z/C*
Co	0.6958 (1)	0.2237 (1)	0.1633 (1)
O(1)	0.4703 (2)	0.2951 (1)	0.1915 (1)
O(2)	0.4371 (3)	0.0387 (2)	0.4078 (1)
O(3)	0.3483 (3)	0.3762 (2)	0.2790 (1)
O(4)	0.3843 (3)	0.0639 (2)	0.3021 (1)
O(5)	0.8214 (2)	0.3743 (1)	0.1875 (1)
N(1)	0.9343 (3)	0.1473 (2)	0.1470 (1)
N(2)	0.7262 (3)	0.1691 (2)	0.2517 (1)
N(3)	0.5536 (3)	0.0821 (2)	0.1368 (1)
N(4)	0.6560 (3)	0.2821 (2)	0.0752 (1)
C(1)	0.4674 (3)	0.3143 (2)	0.2534 (1)
C(2)	0.6297 (3)	0.2599 (2)	0.2931 (1)
C(3)	0.5747 (4)	0.2087 (2)	0.3582 (1)
C(4)	0.4554 (4)	0.0957 (2)	0.3556 (1)
C(5)	0.9290 (4)	0.1515 (3)	0.2647 (1)
C(6)	1.0008 (4)	0.0832 (3)	0.2070 (1)
C(7)	0.4415 (5)	0.1126 (3)	0.0791 (2)
C(8)	0.5452 (6)	0.1929 (4)	0.0369 (1)
Cl	0.0457 (1)	0.3368 (1)	0.4418 (1)
O(6)	0.2076 (4)	0.4143 (3)	0.4387 (1)
O(7)	−0.1059 (4)	0.3993 (3)	0.4103 (1)
O(8)	0.0069 (4)	0.3152 (3)	0.5080 (1)
O(9)	0.0766 (5)	0.2228 (2)	0.4111 (1)
O(10)	0.1461 (3)	0.3865 (2)	0.1296 (1)
O(11A)	0.2422 (8)	0.4836 (6)	0.0191 (2)
O(11B)	0.1619 (8)	0.4966 (5)	0.0057 (2)

[a] The figure in parentheses following each datum is the estimated standard deviation in the last significant figure.

Crystals of all three compounds consist of a cationic cobalt(III) complex, an anion, and either two or three waters of crystallization. Extensive networks of hydrogen bonding, usually involving the

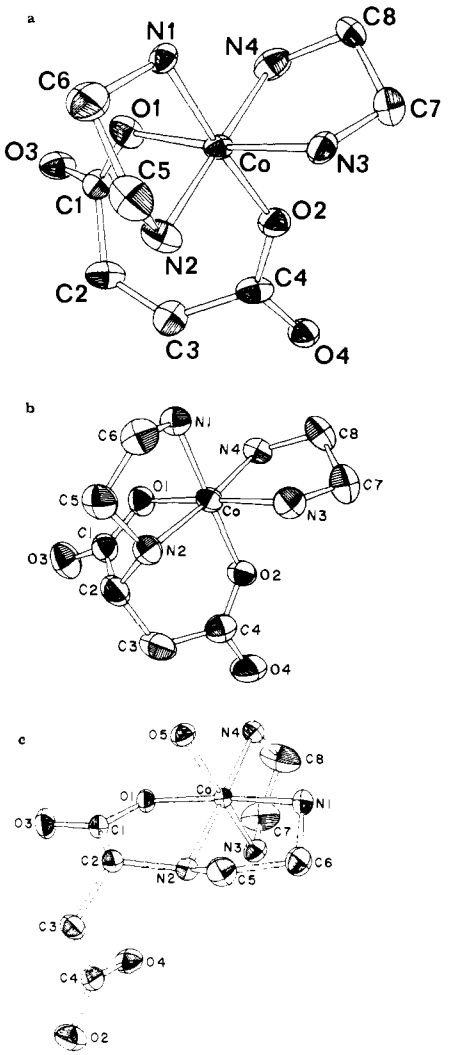

Figure 3. Molecular geometry and atom numbering in Λ-$[Co(en)_2(maleato)]^+$ (a), Δ-*fac*(5,5)-$[Co(en)(R\text{-aea})]^+$ (b), and $[Co(en)(aea)(H_2O)]^+$ (c). The hydrogen atoms have been omitted for clarity, and the thermal ellipsoids have been drawn to include 50% of the probability distribution.

nitrogen atoms, the uncoordinated carboxylate oxygen atoms, the oxygen atoms of the anions, and the waters of crystallization, exist in all three cases.

The cationic complex $[Co(en)_2(maleato)]^+$ closely approximates octahedral geometry with all three ligands bound bidentate. The $(+)_{589}$-isomer has the Λ absolute configuration. One of the most interesting features of the complex is that the seven-membered chelate ring adopts a pseudoboat conformation, which places the olefinic carbon atoms C2 and C3 into close proximity to N2 (d(N2–C2) = 3.15 Å and d(N2–C3) = 3.14 Å). Each carboxylate group and the olefin group are significantly noncoplanar (the dihedral angle between plane O1, O3, C1, C2 and plane C1, C2, C3, C4 is 50°, and the dihedral angle between plane O2, O4, C3, C4 and plane C1, C2, C3, C4 is 36°). The bond lengths and angles within the maleate moiety of $[Co(en)_2(maleato)]^+$ are in excellent agreement with those reported for maleic acid and for maleate salts.[26] In fact, although the C1–C2–C3 and C2–C3–C4 angles of 128.5 (3) and 128.9 (3)°, respectively, are considerably larger than the 120° expected for a trigonally hybridized carbon atom and might be attributed to strain within the chelated maleate ion, similar angle opening has been found for maleic acid itself and for simple maleate salts.[26]

Some information about the conformational lability of the $[Co(en)_2(maleato)]^+$ ion in solution may be gained from the solution NMR data, Figure 4. The olefinic carbon atoms and

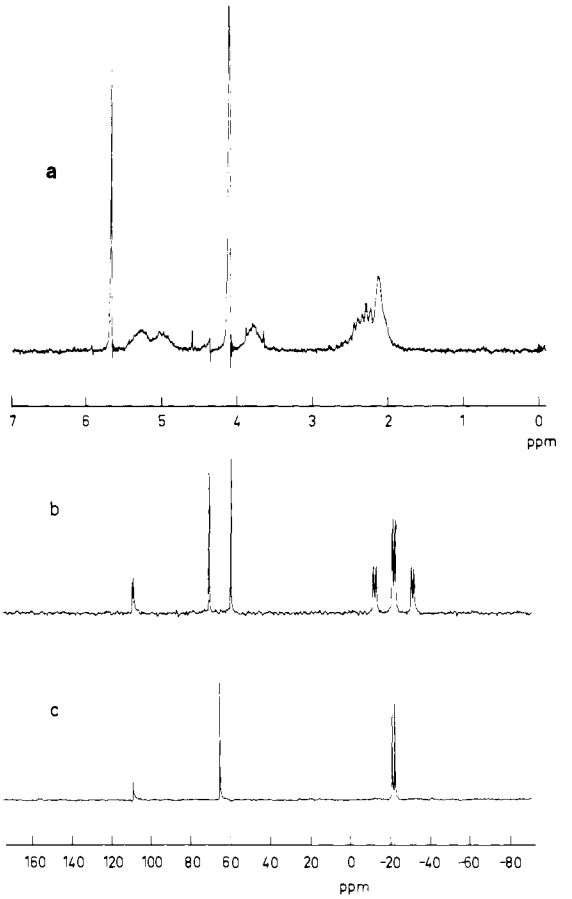

Figure 4. ^1H (a), ^{13}C (without ^1H-decoupling) (b), and ^{13}C (c) NMR spectra of $[Co(en)_2(maleato)]NO_3$ in D_2O. Peak positions in spectrum c are δ 108.7, 64.8, −21.4, and −22.7.

attached protons of the chelated maleate moiety show up as singlet peaks in the ^{13}C NMR (δ 64.8) and ^1H NMR (δ 5.7) spectra, respectively. Only two resonances ascribable to the four carbon atoms of the ethylenediamine ligands are observed in the ^{13}C NMR spectrum. This evidence may indicate an averaging of the complex geometry to C_2 symmetry over the NMR time scale. However, this statement presupposes that under the conditions of measurement splitting of at least one of these resonance peaks into two peaks would be detectable in the event that the complex geometry did not average to C_2, but lower symmetry. If the supposition is correct, the NMR results imply that the maleate chelate ring in $[Co(en)_2(maleato)]^+$ is conformationally flexible in solution and is not locked in the pseudoboat conformation adopted in the solid-state structure of $(+)_{589}$-Λ-$[Co(en)_2(maleato)]PF_6 \cdot 2H_2O$.

The structure of $(-)_{589}$-Δ-*fac*(5,5)-$[Co(en)(R\text{-aea})]^+$ in the crystal confirms the identity of the coordinated *N*-(2-aminoethyl)aspartate molecule. The ligand is coordinated in a quadridentate fashion and gives rise to one seven-membered, one six-membered, and two five-membered chelate rings. The two five-membered rings are attached to the Co(III) ion in a facial mode and thus define the complex as the *fac*(5,5)-isomer according to the nomenclature adopted here. Likewise, the absolute configuration of the complex ion is seen to be Δ because of its relationship to the parent Δ-$[Co(en)_2(maleato)]^+$ ion.

The X-ray crystallographic results indicate that *N*-(2-aminoethyl)aspartate also forms part of the *mer*(5,5)-$[Co(en)(aea)(H_2O)]^+$ complex ion, depicted in Figure 3. Although potentially quadridentate, the amine acidate acts as a tridentate ligand in this instance with the two amino groups and one carboxylate function coordinated to the metal center in a meridional fashion. The other carboxylate group of the aea ligand is not engaged in bonding to the metal ion. Chelated ethylenediamine and one molecule of water occupy the remaining three coordination sites.

(26) James, M. N. G.; Williams, G. J. B. *Acta Crystallogr., Sect. B* **1974**, *30B*, 1249–1257 and references therein.

Table V. Bond Lengths (Å) and Interbond Angles (deg)[a]

atoms	$[Co(en)_2(maleato)]^+$	$[Co(en)(aea)]^+$	$[Co(en)(aea)(H_2O)]^+$
Co-O1	1.917 (2)	1.914 (3)	1.904 (2)
Co-O2	1.905 (3)	1.925 (3)	
Co-O5			1.935 (2)
Co-N1	1.932 (3)	1.943 (3)	1.944 (2)
Co-N2	1.951 (3)	1.951 (3)	1.934 (2)
Co-N3	1.919 (3)	1.946 (4)	1.926 (2)
Co-N4	1.943 (3)	1.946 (4)	1.948 (2)
O1-C1	1.269 (4)	1.284 (5)	1.300 (3)
O2-C4	1.270 (4)	1.279 (5)	1.258 (3)
O3-C1	1.236 (4)	1.246 (7)	1.222 (3)
O4-C4	1.238 (5)	1.235 (5)	1.259 (3)
C1-C2	1.479 (5)	1.521 (8)	1.532 (3)
C2-C3	1.333 (5)	1.514 (6)	1.520 (3)
C3-C4	1.471 (5)	1.513 (7)	1.503 (4)
N1-C6	1.478 (5)	1.470 (7)	1.495 (3)
N2-C2		1.484 (7)	1.492 (3)
N2-C5	1.476 (5)	1.500 (5)	1.489 (3)
N3-C7	1.466 (5)	1.497 (7)	1.464 (4)
N4-C8	1.483 (5)	1.484 (7)	1.477 (4)
C5-C6	1.500 (6)	1.511 (7)	1.510 (4)
C7-C8	1.488 (6)	1.483 (8)	1.456 (5)
O1-Co-O*X*[b]	95.4 (1)	90.0 (1)	88.2 (1)
O1-Co-N1	87.7 (1)	91.3 (1)	172.1 (1)
O1-Co-N2	96.0 (1)	83.4 (2)	85.0 (1)
O1-Co-N3	172.6 (1)	174.8 (2)	88.0 (1)
O1-Co-N4	87.1 (1)	91.0 (2)	92.7 (1)
O*X*-Co-N1[b]	176.4 (1)	178.7 (2)	90.1 (1)
O*X*-Co-N2[b]	95.5 (1)	93.8 (1)	88.6 (1)
O*X*-Co-N3[b]	85.2 (1)	85.3 (1)	175.2 (1)
O*X*-Co-N4[b]	86.8 (1)	88.7 (1)	91.2 (1)
N1-Co-N2	85.8 (1)	86.6 (1)	87.3 (1)
O3-C1-C2	116.5 (3)	120.4 (4)	120.9 (2)
O2-C4-O4	121.7 (3)	121.2 (4)	125.0 (2)
O2-C4-C3	121.3 (3)	120.7 (3)	116.6 (2)
O4-C4-C3	117.0 (3)	118.1 (4)	118.5 (2)
C1-C2-C3	128.5 (3)	112.3 (4)	114.0 (2)
C1-C2-N2		106.5 (3)	107.9 (2)
C3-C2-N2		109.6 (4)	113.6 (2)
C2-C3-C4	128.9 (3)	116.2 (4)	115.5 (2)
Co-N2-C2		103.2 (3)	107.3 (1)
Co-N2-C5	109.5 (2)	108.8 (2)	107.3 (1)
N1-Co-N3	91.5 (1)	93.5 (2)	94.0 (1)
N1-Co-N4	91.7 (1)	91.1 (1)	95.0 (1)
N2-Co-N3	91.3 (1)	99.0 (2)	94.0 (1)
N2-Co-N4	176.0 (2)	173.9 (2)	177.7 (1)
N3-Co-N4	85.6 (1)	86.7 (2)	86.0 (1)
Co-O1-C1	129.6 (2)	112.4 (3)	113.8 (1)
Co-O2-C4	133.3 (2)	128.6 (3)	
O1-C1-O3	120.8 (3)	123.9 (5)	123.1 (2)
O1-C1-C2	122.7 (3)	115.6 (4)	115.9 (2)
C2-N2-C5		112.9 (3)	116.7 (2)
N2-C5-C6	106.2 (3)	107.8 (4)	105.8 (2)
C5-C6-N1	107.7 (3)	106.6 (4)	108.6 (2)
Co-N1-C6	109.6 (2)	109.2 (2)	108.8 (2)
Co-N3-C7	109.0 (2)	108.4 (4)	109.1 (2)
N3-C7-C8	106.8 (4)	108.0 (4)	110.3 (3)
C7-C8-N4	106.7 (3)	109.2 (4)	110.6 (3)
Co-N4-C8	110.0 (2)	109.8 (3)	110.7 (2)

[a] The figure in parentheses following each datum is the estimated standard deviation in the last significant figure. [b] $X = 2$ for $[Co(en)_2(maleato)]^+$ and $[Co(en)(aea)]^+$ and $X = 5$ for $[Co(en)(aea)(H_2O)]^+$.

The three ligating groups together with adjoining ligand segments of aea form a system of two linked five-membered chelate rings. This geometry allows the complex to be described as the *mer*(5,5)-isomer. The conformation of the Co-O1-C1-C2-N2 chelate ring is such that the carboxylatomethyl substituent on C2 is equatorial to the ring. This orientation would seem to involve the least steric strain as compared to the conformation where the substituent is axial to the ring. As a consequence, the proton in the secondary amine group at N2 of coordinated aea is syn to the carboxylatomethyl substituent on the adjacent carbon atom C2. Both the N2–H proton and the carboxylatomethyl substituent are on the remote (anti) side of the meridional plane (defined by O1, N2, N1) relative to the coordinated aqua ligand, O5.

Comparison of $(-)_{589}$-Δ-*fac*(5,5)-$[Co(en)(R\text{-aea})]^+$ and *mer*-(5,5)-$[Co(en)(aea)(H_2O)]^+$ offers an interesting insight into the geometries of the facial vs. meridional arrangements of the five-membered chelate rings of the *N*-(2-aminoethyl)aspartate ligand. Although the facial arrangement appears to be the thermodynamically more stable one (vide infra), there is virtually no difference in bond lengths and bond angles (Table V) within the chelate rings Co-O1-C1-C2-N2 and Co-N2-C5-C6-N1 in *fac*(5,5)-$[Co(en)(aea)]^+$ and the corresponding rings in $[Co(en)(aea)(H_2O)]^+$. The O1–Co–N1 angle in $[Co(en)(aea)(H_2O)]^+$, however, has closed slightly to 172.1 (1)°, and the C2–N2–C5 angle has opened to 116.7 (2)° from the value of 112.9 (3)° found in *fac*(5,5)-$[Co(en)(aea)]^+$, which is evidence of some

Table VI. Pseudo-First-Order Rate Constants for Reaction of *fac*(5,5)-[Co(en)(aea)]Br[a] with NaOH (25 °C, μ = 1.0 M ($NaClO_4$))

[NaOH], M	$k_{obsd} \times 10^3$,[b] s^{-1}	[NaOH], M	$k_{obsd} \times 10^3$,[b] s^{-1}
0.025	3.9 ± 0.2	0.25	5.63 ± 0.05
0.035	4.1 ± 0.2	0.30	6.03 ± 0.09
0.050	4.4 ± 0.2	0.40	6.74 ± 0.07
0.10	4.6 ± 0.2	0.50	7.32 ± 0.04
0.15	4.95 ± 0.04	0.75	8.3 ± 0.2
0.20	5.37 ± 0.04	1.00	8.9 ± 0.2

[a] Concentration of complex 3.5 mM. [b] Values obtained as mean of quadruplicates.

strain in the meridional arrangement of the chelate rings.

The bond lengths and angles within the *N*-(2-aminoethyl)aspartate ligands in $[Co(en)(aea)]^+$ and $[Co(en)(aea)(H_2O)]^+$ agree very well with those reported for aspartic acid,[27,28] aspartate salts[29] and Co(III) complexes,[30-32] the Co(III) complex of *N*-(2-pyridylmethyl)aspartate,[33] and *N,N'*-ethylenediaminedisuccinic acid[34] and its Co(III) complex.[35] As expected, the C–O bond distances for the coordinated oxygen atoms of the carboxylate groups are significantly longer than the C–O distances involving the free oxygens. The C2–C3–C4 angles of 116.2 (4) Å in $[Co(en)(aea)]^+$ are both larger than the ideal tetrahedral value of 109°, a feature also found in both complexes and free aspartates.[29-32] The Co–O(carboxylate) bond lengths within all three complexes range from 1.904 (2) to 1.925 (3) Å with an average of 1.913 Å. The Co–N bond lengths average 1.940 Å and range from 1.919 (3) to 1.951 (3) Å.

The bond lengths and angles within the ethylenediamine ligands are normal.[36]

Relevant results for the anions of the three structures are available as Supplementary Material. Bond lengths and angles in the bromocamphorsulfonate molecule are in excellent agreement with those reported elsewhere,[37,38] while the bond lengths and angles for ClO_4^- are also normal. However, due to disordering there are rather wide variations in the P–F distances and the F–P–F angles in the PF_6^- group of the $(+)_{589}$-Λ-$[Co(en)_2(maleato)]PF_6 \cdot 2H_2O$ structure.

Kinetic and Product Distribution Studies. Reaction of *fac*-(5,5)-[Co(en)(aea)]Br with NaOH. With NaOH in excess (>7-fold) over complex, the change in optical density was followed at 410 nm. Presumably due to subsequent, but much slower, reactions, no well-defined infinite time absorption reading (A_∞) for the studied reaction was obtained. However, the experimental data of absorption readings (A_t) at different times (t) could be adequately fitted to the function (1) over $>3t_{1/2}$ by a standard computer iteration program. In the fitting procedure A_0, A_∞,

$$A_t = (A_0 - A_\infty) \exp(-k_{obsd}t) + A_\infty \quad (1)$$

and k_{obsd} (the first-order rate constant) were treated as variables. The rate constants thus obtained for a range of NaOH concentrations are given in Table VI. No simple relationship between k_{obsd} and $[OH^-]$ was found. Also, the observed change in optical density, $A_0 - A_\infty$, associated with the reaction varied with $[OH^-]$, displaying a maximum at $[OH^-] \sim 0.45$ M.

Table VII. Pseudo-First-Order Rate Constants[a] for Reaction of *mer*(5,5)-[Co(en)(aea)]ClO_4[b] with OH^- (25 °C, μ = 1.0 M ($NaClO_4$))

	400 nm[c]		460 nm[d]	510 nm[c]	
$[OH^-]$	k_1, s^{-1}	k_2, s^{-1}	k_1, s^{-1}	k_1, s^{-1}	k_2, s^{-1}
0.025	0.09	0.04	0.08	0.09	0.03
0.050	0.18	0.04	0.18	0.18	0.05
0.100	0.36	0.05	0.37	0.35	0.05
0.200	0.71	0.04	0.73	0.70	0.07

[a] All values obtained are means of triplicates. Estimated standard deviations less than ±0.01 s^{-1}. [b] Concentration of complex: 1 mM for runs at 400 nm and 510 nm and 2 mM for those at 460 nm. [c] Rate constants obtained from fitting function $A_t - A_\infty = A_1\exp(-k_1t) + A_2\exp(-k_2t)$. [d] Rate constants obtained from first-order rate plots.

Although interesting in its own right, this investigation of the reaction of *fac*(5,5)-$[Co(en)(aea)]^+$ with OH^- is as yet incomplete. For example, no product analysis has been carried out, and the unusual dependence of the rate with $[OH^-]$ does not imply any obvious explanation. However, the lack of understanding of these particular aspects does not influence the understanding of the remaining chemistry, but the results reported are pertinent to later arguments.

Reaction of *mer*(5,5)-[Co(en)(aea)]ClO_4 with OH^- in Water. (i) Kinetics. The change in optical density was followed in solutions with excess OH^- (>20-fold) over *mer*(5,5)-[Co(en)(aea)]ClO_4 at three different wavelengths (400, 460, and 510 nm). The optical density change at 460 nm followed first-order kinetics, all plots of log ($A_t - A_\infty$) vs. time being linear for at least 3 half-lives. The derived rate constants are given in Table VII.

For runs at 400 and 510 nm, plots of log ($A_t - A_\infty$) vs. time were nonlinear and showed curvature indicative of a consecutive kinetic process. The sets of data (A_t,t) from each kinetic run are represented by eq 2, and the kinetic data were fitted by a standard

$$A_t - A_\infty = A_1 \exp(-k_1t) + A_2 \exp(-k_2t) \quad (2)$$

least-squares computer program taking A_1, k_1, A_2, and k_2 as the parameters with k_1 the larger of the two rate constants. The fitting procedure gave calculated errors of less than ±5% for the values of k_1 and k_2 in all instances. Table VII lists the mean values from triplicate runs.

Linear plots of k_1 vs. $[OH^-]$ passing through the origin were observed at all wavelengths investigated. The data thus obeyed the rate law $k_1 = k[OH^-]$. The value for k calculated by a linear least-squares procedure from the k_1 values in Table VII is 3.6 ± 0.1 M^{-1} s^{-1} at all three wavelengths.

The values obtained for k_2 are essentially identical at 400 and 510 nm and do not vary significantly with $[OH^-]$; k_2 = 0.05 ± 0.01 s^{-1}. Although the reactions are consecutive, their sequence is undetermined by the kinetic data alone.[39]

(ii) Product Distribution. The number and identity of products and intermediates formed in the base-hydrolysis reaction of *mer*(5,5)-$[Co(en)(aea)]^+$ were investigated by ^{13}C NMR spectroscopy. When a sample of *mer*(5,5)-$[Co(en)(aea)]O_3SCF_3$ was treated in 0.4 M NaOD and the solution acidified to pD ~2 after 5 min ($>20 \times t_{1/2}$ for the slowest step), the ^{13}C NMR spectrum of the resulting solution coincided with that of *mer*(5,5)-$[Co(en)(aea)(H_2O)]ClO_4 \cdot 2H_2O$ dissolved in D_2O at pD ~2–3 (DCl).

When the reaction was quenched with acid after only ~3 s, several sets of signals appeared in the ^{13}C NMR spectrum of the quenched solution. In addition to resonances attributable to the reactant (A) and the end product *mer*(5,5)-$[Co(en)(aea)(H_2O)]^+$ (C), a total of eight new peaks were observed (Table VIII). These

(27) Rao, S. T. *Acta Crystallogr., Sect. B* **1973**, *29B*, 1718–1720.
(28) Derissen, J. L.; Endeman, H. J.; Peerdeman, A. F. *Acta Crystallogr., Sect. B* **1968**, *24B*, 1349–1354.
(29) Bhat, T. N.; Vijayan, M. *Acta Crystallogr., Sect. B* **1976**, *32B* 891–895.
(30) Oonishi, I.; Shibata, M.; Marumo, F.; Saito, Y. *Acta Crystallogr., Sect. B* **1973**, *29B*, 2448–2455.
(31) Oonishi, I.; Sato, S.; Saito, Y. *Acta Crystallogr., Sect. B* **1975**, *31B*, 1318–1324.
(32) Sekizaki, M. *Bull. Chem. Soc. Jpn.* **1978**, *51*, 1991–1995.
(33) Meiske, L. A.; Jacobson, R. A.; Angelici, R. J. *Inorg. Chem.* **1980**, *19*, 2028–2034.
(34) Scarbrough, F. F.; Voet, D. *Acta Crystallogr., Sect. B.* **1976**, *32B*, 2715–2717.
(35) Pavelcik, F.; Majer, J. *Acta Crystallogr., Sect. B.* **1978**, *34B*, 3582–3585.
(36) Templeton, D. H.; Zalkin, A.; Ruben, H. W.; Templeton. L. K. *Acta Crystallogr., Sect. B.* **1979**, *35B*, 1608–1613.
(37) Wunderlich, J. A. *Acta Crystallogr.* **1967**, *23*, 846–855.
(38) Kuramoto, M.; Kushi, Y.; Yoneda, H. *Bull. Chem. Soc. Jpn.* **1978**, *51*, 3196–3202.
(39) Jackson, W. G.; Harrowfield, J. MacB.; Vowles, P. D. *Int. J. Chem. Kinet.* **1977**, *9*, 535–548.

Table VIII. ^{13}C NMR Data for Product Mixture from Reaction of *mer*(5,5)-$[Co(en)(aea)]O_3SCF_3$ with OD^- in D_2O. Chemical Shifts in ppm (relative to 1,4-dioxane)

mixture[a]	*mer*(5,5)-$[Co(en)(aea)]^+$ (A)	*mer*(5,5)-$[Co(en)(aea)(H_2O)]^+$ (C)	new species (B)
117.7	118.0	117.8	
116.7			116.7
109.8	109.5		
108.2		108.4	
107.8			107.8
−5.3			−5.3
−6.5		−6.3	
−7.3	−7.3		
−15.1			−15.1
−16.7		−16.6	
−20.5	−20.3	−20.3	−20.5
−21.0	−20.5	−20.9	−21.0
−21.1	−21.3		
−22.9		−22.6	
−23.3			−23.3
−23.8	−23.9		
−32.7		−32.4	
−33.3			−33.3
−33.4	−33.4		

[a] Four additional peaks (δ = 84.7, 63.7, 42.5, and 21.4) were ascribed to the $CF_3SO_3^-$ ion.

peaks were ascribed to a reaction intermediate B whose existence is consistent with the kinetic results presented above. If, in the observed kinetic pattern, the faster step precedes the slower, a build-up of an intermediate should take place. A peak concentration of this intermediate should be seen after an appropriate reaction time as defined by the kinetic parameters. Each of the new resonance peaks ascribed to B was located close ($\Delta\delta$ <1.5) to a corresponding peak of *mer*(5,5)-$[Co(en)(aea)(H_2O)]^+$. A close structural relationship of the intermediate B and the latter species with respect to the environment of the ligand carbon atoms is therefore implied.

An estimate of the relative amounts present of *mer*(5,5)-$[Co(en)(aea)]^+$ (A), the intermediate (B), and *mer*(5,5)-$[Co(en)(aea)(H_2O)]^+$ (C) in reaction mixtures quenched at different times can be obtained from an integration over relevant resonance peaks in the ^{13}C NMR spectra of the mixtures. A group of well-separated peaks at −7.3 (A), −6.3 (C), and −5.3 (B) ppm were chosen for the analysis. Assuming that these three peaks are due to the same carbon atom of aea in the three complex isomers, it is reasonable to assume further that the area under each peak would be essentially the same for identical concentrations of the three complex species. Their relative amounts were determined on this basis, and the results for reaction mixtures quenched at invervals are represented graphically in Figure 5. The spectra were always recorded immediately after quenching, but a spectrum of the sample from the 1.6-s experiment recorded again 17 h later was essentially unchanged.

The results in Figure 5 combined with the kinetic results reported earlier preclude the following mechanism:

$$A \xrightarrow[k = 3.6\ M^{-1}\ s^{-1}]{OH^-} B \xrightarrow[k_2 = 0.05\ s^{-1}]{} C$$

If this obtained the intermediate B would constitute 88% of all complex species[40] after 3 s of reaction, which is clearly not found. However, the combined results for the system are adequately represented by the reaction paths:

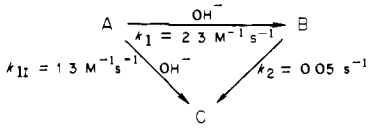

(40) Wilkins, R. G. "The Study of Kinetics and Mechanism of Reactions of Transition Metal Complexes"; Allyn and Bacon: Boston, 1974; p 22.

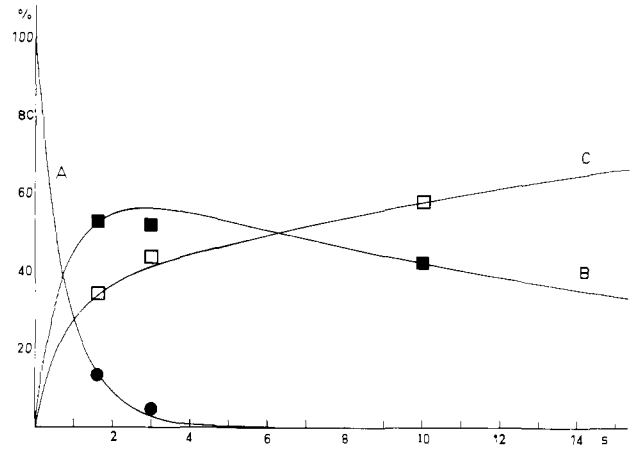

Figure 5. Distribution of *mer*(5,5)-$[Co(en)(aea)]^+$ (A, ●), the intermediate (B, ■), and *mer*(5,5)-$[Co(en)(aea)(H_2O)]^+$ (C, □). The theoretical distribution curves for species A, B, and C were obtained as outlined in the test and are represented by solid lines.

Table IX. Rate Constants for Reaction of $[Co(en)_2(maleato)]ClO_4$[a] with OH^- (25 °C, μ = 1.0 M ($NaClO_4$))

[NaOH], M	$k_{obsd} \times 10^3$, s^{-1}	[NaOH], M	$k_{obsd} \times 10^3$, s^{-1}
0.025	9.6 ± 0.4[c]	0.200	87 ± 2[b]
0.050	18.9 ± 0.3[b]	0.300	134 ± 2[b]
0.100	42 ± 2[c]	0.400	178 ± 4[c]

[a] Concentration of complex 1.0 mM. [b] Mean of triplicates. [c] Mean of quadruplicates.

The reagent A reacts to give B and C in two parallel reactions, which are both first order in $[OH^-]$, with rate constants k_1 = 2.3 $M^{-1}\ s^{-1}$ and k_{II} = 1.3 $M^{-1}\ s^{-1}$, respectively. The sum of k_1 and k_{II} is 3.6 $M^{-1}\ s^{-1}$ in accordance with the observed kinetic behavior. The intermediate B subsequently reacts to give C in a reaction that is independent of $[OH^-]$ and has the rate constant k_2 = 0.05 s^{-1}. The distribution functions represented in Figure 5 were calculated on the basis of this kinetic pattern applying corrections assuming that 1 mol of OH^- is consumed per mol of A. Details of the calculations are given in an Appendix submitted as Supplementary Material.

Reaction of $[Co(en)_2(maleato)]ClO_4$ with OH^- in Water. (i) Kinetics. Under conditions where NaOH was in excess (>25-fold) over $[Co(en)_2(maleato)]^+$ the changes in optical density at 495 nm were followed. Plots of log $(A_t - A_\infty)$ against time were linear for at least 3 half-lives. Rate constants for a range of hydroxide ion concentrations are given in Table IX, and a plot of k_{obsd} vs. $[OH^-]$ is linear and passes through the origin. The simplest rate law consistent with this data is $k_{obsd} = k[OH^-]$, and the mean value of k calculated from the data of Table IX is 0.45 ± 0.01 $M^{-1}\ s^{-1}$.

(ii) Product Distribution Analysis. Table X lists the products of the aqueous base treatment of $[Co(en)_2(maleato)]^+$ in order of elution from the chromatographic separation on SP Sephadex C-25 resin. Unreacted $[Co(en)_2(maleato)]^+$ (band 2) and *mer*-(5,5)-$[Co(en)(aea)(H_2O)]^+$ (band 4) were both characterized by their visible absorption and rotary dispersion spectra in an experiment using chiral starting material. The singly charged cationic complexes constituting bands 1 and 3 both liberated maleate anion upon decomposition with Na_2S. When chiral starting material was used, the eluate of band 3 was optically active. The rotary dispersion spectrum of this band had a maximum at 520 nm and a maximum of opposite sign at 440 nm. The visible absorption spectrum (ϵ_{max} 117, 494 nm; ϵ_{max} 87, 358 nm) resembled that reported for *cis*-$[Co(en)_2(H_2O)(OOCCH_3)]^{2+}$ (ϵ_{max} 113, 495 nm; ϵ_{max} 80, 358 nm).[24] The eluate of band 1 showed no optical activity when chiral reagent complex had been used, and the spectrum (ϵ_{max} 50, 543 nm; ϵ_{max} 32, 452 nm; ϵ_{max} 69, 356 nm) resembled that reported for *trans*-$[Co(en)_2(H_2O)(OOCCH_3)]^{2+}$ (ϵ_{max} 51.3, 543 nm; ϵ_{max} 32.4, 445 nm; ϵ_{max} 66.1, 355 nm).[41] The evidence indicates that the complex species are

Table X. Products[a] (%) from Reaction of $[Co(en)_2(maleato)]ClO_4$ with OH^- at 25 ± 1 °C

band[b]	complex	0.5 M NaOH at reaction time = 3 s ($t_{1/2}$)	0.5 M NaOH at reaction time = 30 s ($10t_{1/2}$)	0.25 M NaOH at reaction time = 6 s ($t_{1/2}$)	0.25 M NaOH at reaction time = 60 s ($10t_{1/2}$)
1	*trans*-$[Co(en)_2(H_2O)(maleato)]^+$	28.1	35.4	27.7	42.2
2	$[Co(en)_2(maleato)]^+$	40.7	5.3	44.4	6.4
3	*cis*-$[Co(en)_2(H_2O)(maleato)]^+$	17.1	36.9	16.0	29.0
4	*mer*(5,5)-$[Co(en)(aca)(H_2O)]^+$	11.3	18.7	10.5	20.0
5	$[Co(en)_2(H_2O)_2]^{3+}$	2.8	3.7	1.4	2.4
ratio	4/(1+3+5)	0.235	0.246	0.233	0.271
				av 0.25 ± 0.02	

[a] Recovery better than 98% in all experiments. [b] In order of elution on SP-Sephadex C-25 with 0.1 M citrate buffer, pH 3.8 as eluant.

cis (band 3) and trans (band 1) isomers of $[Co(en)_2(H_2O)(maleato)]^+$, where the maleate dianion is bound as a monodentate.

Band 5, which accounts for less than 4% of the products, was assumed to contain *cis*- and *trans*-$[Co(en)_2(H_2O)_2]^{3+}$ on the basis of its much higher charge compared with the other products and the likely chemistry. For example, it is reasonable to expect $[Co(en)_2(H_2O)(maleato)]^+$ to slowly hydrolyze[42] in the basic conditions to give $[Co(en)_2(OH)_2]^+$, which, under the conditions of the chromatographic separation (pH 3.8), would be present essentially in the protonated form $[Co(en)_2(H_2O)_2]^{3+}$ (in 1 M $NaNO_3$: 25 °C trans, pK_a = 4.45; cis, pK_a = 6.06).[43]

The *fac*(5,5)-$[Co(en)(aea)]^+$ isomer would have been detected had it been formed in the reaction of $[Co(en)_2(maleato)]^+$ with OH^-. A sample of *fac*(5,5)-[Co(en)(aea)]Br was treated in 0.25 M NaOH for 60 s in an identical manner to the treatment of $[Co(en)_2(maleato)]ClO_4$ salt, Table X, and subsequent chromatography showed the orange reactant to be unaltered. When a mixture of *fac*(5,5)-[Co(en)(aea)]Br and $[Co(en)_2(maleato)]ClO_4$ was treated with base and chromatographed similarly, the orange-colored band of *fac*(5,5)-$[Co(en)(aea)]^+$ appeared on the chromatography column after band 2 of $[Co(en)_2(maleato)]^+$ but before band 3 of *cis*-$[Co(en)_2(H_2O)(maleato)]^+$. All three bands were clearly separated. However, when $[Co(en)_2(maleato)]ClO_4$ alone was subjected to the base treatment and the products chromatographed, no orange-colored band corresponding to *fac*(5,5)-$[Co(en)(aea)]^+$ was detected.

The product distribution results, listed in Table X, were obtained in 0.25 or 0.50 M NaOH and for each base concentration with reaction times of $\sim t_{1/2}$ or $\sim 10t_{1/2}$. In all instances, the mole ratio α = {*mer*(5,5)-$[Co(en)(aea)(H_2O)]^+$}/({*cis*- + *trans*-$[Co(en)_2(H_2O)(maleato)]^+$} + {$[Co(en)_2(H_2O)_2]^{3+}$}) was essentially constant (0.25 ± 0.01). The same trend was found for the same reaction (>10 × $t_{1/2}$) in $NaHPO_4$-buffer pH 11.5 of differing concentrations (0.5 M, α 0.2; 0.25 M, α 0.2). The observed constancy of α for reaction times $t_{1/2}$ and $10t_{1/2}$ is consistent with two independent reaction paths for the reaction of $[Co(en)_2(maleato)]^+$ with base: one path leading to *mer*(5,5)-[Co(en)(aea)(OH)] with k_1 = 0.09 M^{-1} s^{-1} and the other path yielding a mixture of *cis*- and *trans*-$[Co(en)_2(OH)(maleato)]$ (which subsequently hydrolyzed to $[Co(en)_2(OH)_2]^+$) with k_2 = 0.36 M^{-1} s^{-1} for the rate-controlling reaction.

Reaction of $[Co(en)_2(maleato)]ClO_4$ with Base in Liquid NH_3 or Me_2SO. Chromatography of the product mixture from the reaction of $(+)_{589}$-Λ-$[Co(en)_2(maleato)]^+$ with ethanolamine in Me_2SO revealed a maximum of three bands. Occasionally a minor leading band (1) was identified as unreacted starting material on the basis of its absorption, RD, and CD spectra. The trailing band (3) was identified likewise as *mer*(5,5)-$[Co(en)(aea)(H_2O)]^+$. The major band (2) chromatographed as *fac*(5,5)- or *mer*(5,5)-$[Co(en)(aea)]^+$ and the CD spectrum of the eluate was consistent with a combination of the individual spectra of the two isomers

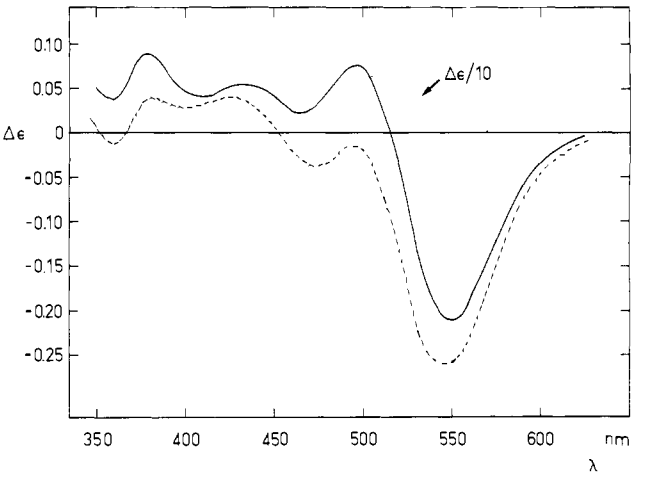

Figure 6. CD spectra of $(-)_{589}$-*mer*(5,5)-$[Co(en)(aea)]ClO_4$ (---), $(+)_{589}$-*fac*(5,5)-$[Co(en)(aea)]ClO_4$ (···, × $^1/_{10}$), and a putative mixture (produced from $(+)_{589}$-$[Co(en)_2(maleato)]ClO_4$ in Me_2So) thereof (—). Solvent: 0.50 M $NaClO_4$/0.05 M $HClO_4$.

$(-)_{589}$-Λ-*mer*(5,5)-$[Co(en)(R\text{-}aea)]^+$ and $(+)_{589}$-Λ-*fac*(5,5)-$[Co(en)(S\text{-}aea)]^+$ (Figure 6). All attempts at separating these two isomers by chromatographic techniques proved unsuccessful, and the amounts present of each isomer in the eluate were assessed on the basis of the CD spectrum of the eluate. The basis for this assessment will now be outlined. Assuming that the CD of the isomeric mixture can be regarded as a simple superposition of the individual CD contributions from the chiral species, then for any wavelength λ (1-cm cell), eq 3 would apply. In the equation,

$$\Delta A_\lambda = [\Delta\epsilon(A/\lambda)a + \Delta\epsilon(B/\lambda)(1 - a)]c \qquad (3)$$

ΔA_λ represents the absorption difference between left and right circularly polarized light of the binary mixture containing A and B with $[A] = ac$ and $[B] = (1 - a)c$; $\Delta\epsilon(A/\lambda)$ and $\Delta\epsilon(B/\lambda)$ are the molar CD for A and B, respectively. Rearranging (3) yields (4), where the left-hand side is a constant for any given λ and can be calculated when the individual CD spectra of A and B are known. If the above assumption holds and ΔA_λ is determined

$$\frac{\Delta\epsilon(B/\lambda)}{\Delta\epsilon(A/\lambda) - \Delta\epsilon(B/\lambda)} = \frac{\Delta A_\lambda}{\Delta\epsilon(A/\lambda) - \Delta\epsilon(B/\lambda)}\frac{1}{c} - a \qquad (4)$$

experimentally on a mixture of A and B in unknown concentrations, a plot of $\Delta\epsilon(B/\lambda)/(\Delta\epsilon(A/\lambda) - \Delta\epsilon(B/\lambda))$ vs. $\Delta A_\lambda/(\Delta\epsilon(A/\lambda) - \Delta\epsilon(B/\lambda))$ for a set of different wavelengths λ should ideally describe a straight line according to (4). Values for the unknowns c (=total concentration of chiral species A and B) and a (=proportion of A) can be obtained from the slope (=c^{-1}) and the intercept (=$-a$), respectively. An analogous analysis may be carried out by using the RD spectrum. The analysis based on the CD spectrum was carried out for sets of data at 10 different wavelengths (570, 560, 550, 510, 500, 490, 470, 430, 380, and 360 nm), which were selected so that the values for $\Delta\epsilon(A/\lambda)$ and $\Delta\epsilon(B/\lambda)$ were optimally different and accurately determined. In this respect the CD spectrum proved to be superior to the RD spectrum as a basis for the analysis, mainly because of the com-

(41) Carunchio, V.; Illuminati, G.; Ortaggi, G. *Inorg. Chem.* **1967**, *6*, 2168–2171.

(42) The rate constant for base hydrolysis of *cis*-$[Co(en)_2(OH)(OOCCH_3)]^+$ is 81.5 × 10^{-4} M^{-1} s^{-1} and for *cis*-$[Co(en)_2(OOCCH_3)_2]^+$ is 241 × 10^{-4} M^{-1} s^{-1} at 25 °C.[41]

(43) Bjerrum, J.; Rasmussen, S. E. *Acta Chem. Scand.* **1952**, *6*, 1265–1284.

Table XI. Product Distributions for the Reactions of $(+)_{589}$-$[Co(en)_2(maleato)]ClO_4$ with Base

	solvent: Me_2SO[a]		solvent: liquid NH_3[b]	
	I	II[c]	III	IV[c]
band 1				
$(+)_{589}$-$[Co(en)_2(maleato)]^+$ (by AAS), mmol	0	0	0	0.014
band 2				
$(-)_{589}$-*mer*(5,5)- and $(+)_{589}$-*fac*(5,5)-$[Co(en)(aea)]^+$:				
total amount (by AAS), mmol	0.238	0.253	0.210	0.230
total amount (from "CD-plot"), mmol	0.238 (2)	0.250 (4)	0.208 (2)	0.234 (2)
$\%(-)_{589}$-*mer*(5,5)-$[Co(en)(aea)]^+$ in band ("CD-plot")	86.0 (3)	86.3 (5)	94.6 (3)	93.8 (4)
$(+)_{589}$-*fac*(5,5)-$[Co(en)(aea)]^+$, mmol	0.033	0.034	0.011	0.015
$(-)_{589}$-*mer*(5,5)-$[Co(en)(aea)]^+$, mmol	0.205	0.216	0.197	0.219
band 3				
$(-)_{589}$-*mer*(5,5)-$[Co(en)(aea)(OH_2)]^+$ (by AAS), mmol	0.109	0.112	0.136	0.122
$(-)_{589}$-*mer*(5,5)-$[Co(en)(aea)]^+$, total amount, mmol	0.314	0.328	0.333	0.341
$(+)_{589}$-*fac*(5,5)-$[Co(en)(aea)]^+$, % of total products	9.5	9.4	3.2	4.2

[a] Base: $H_2NCH_2CH_2OH$. [b] Base: $NaNH_2$. [c] $(-)_{589}$-$[Co(en)_2(maleato)]ClO_4$ used as reagent; all products of opposite chirality to that given in entry.

paratively higher sensitivity of the CD technique, given the available instrumentation and the CD and RD spectra of the relevant complexes (Figure 6). Experimental ΔA_λ values for the eluate of band 2 of the chromatographic product separation, as well as relevant $\Delta\epsilon_\lambda$ values for $(-)_{589}$-*mer*(5,5)-$[Co(en)(aea)]^+$ and $(+)_{589}$-*fac*(5,5)-$[Co(en)(aea)]^+$, respectively, are given in Table 27, which is available as Supplementary Material. When $(+)_{589}$-Λ-$[Co(en)_2(maleato)]^+$ was assumed to yield a mixture of $(-)_{589}$-Λ-*mer*(5,5)-$[Co(en)(R\text{-}aea)]^+$ (A) and $(+)_{589}$-Λ-*fac*(5,5)-$[Co(en)(S\text{-}aea)]^+$ (B), plots of $\Delta\epsilon(B/\lambda)/(\Delta\epsilon(A/\lambda) - \Delta\epsilon(B/\lambda))$ vs. $\Delta A_\lambda/(\Delta\epsilon(A/\lambda) - \Delta\epsilon(B/\lambda))$ for sets of different λ values were linear. This linearity is consistent with the assumptions implied in eq 3. When other combinations of chiralities for *mer*(5,5)- and *fac*(5,5)-$[Co(en)(aea)]^+$ were assumed, the resulting plots were not linear. Values for the total amount of chiral complexes ($=c \times$ volume) in band 2 as well as the proportion (a) of $(-)_{589}$-*mer*(5,5)-$[Co(en)(aea)]^+$, as obtained from the linear plot, appear in Table XI. The table also lists the results when $(-)_{589}$-$[Co(en)_2(maleato)]ClO_4$ was employed as the reagent as well as the results obtained when liquid NH_3 was the solvent. For all fractions the total amount of Co was determined by atomic absorption spectroscopy (AAS). The total amounts of complex detected in the eluates of band 2 by the AAS technique are essentially identical with the amounts determined from the CD spectral analyses in each case. Since the latter technique only detects the amount of complex species actually contributing to the CD, the excellent agreement for the two independent methods indicates that essentially no racemic fractions of Co complexes were present in the eluates of band 2. The implication is that the reaction of $(+)_{589}$-Λ-$[Co(en)_2(maleato)]^+$ to give a mixture of $(-)_{589}$-Λ-*mer*(5,5)-$[Co(en)(R\text{-}aea)]^+$ and $(+)_{589}$-Λ-*fac*(5,5)-$[Co(en)(S\text{-}aea)]^+$ proceeds near quantitatively without change in configuration at the metal ion in both Me_2SO and liquid NH_3.

The presence of some *mer*(5,5)-$[Co(en)(aea)(H_2O)]^+$ (band 3) among the products could not be avoided. This complex was assumed to arise as a hydrolysis product from *mer*(5,5)-$[Co(en)(aea)]^+$ in the basic reaction media since no serious attempt was made to exclude moisture. A separate set of experiments was consistent with this assumption. If $(-)_{589}$-*mer*(5,5)-$[Co(en)(aea)]ClO_4 \cdot 0.5H_2O$ was treated with $NaNH_2$ in liquid NH_3 identically to the experiments using $[Co(en)_2(maleato)]ClO_4$, the subsequent chromatographic separation of products revealed two orange-colored bands. These bands correspond to bands 2 and 3 above, band 2 now containing unreacted $(-)_{589}$-*mer*(5,5)-$[Co(en)(aea)]^+$ only and none of the *fac*(5,5)-isomer. By contrast, if $(+)_{589}$-Λ-*fac*(5,5)-$[Co(en)(aea)]ClO_4 \cdot 1.5H_2O$ was subjected to the same treatment, only a single band of unreacted complex was observed. These results indicate that the content of band 3 arises only from hydrolysis of *mer*(5,5)-$[Co(en)(aea)]^+$ and not from hydrolysis of *fac*(5,5)-$[Co(en)(aea)]^+$. Taking this fact into account, the total amounts of *mer*(5,5)- and *fac*(5,5)-$[Co(en)(aea)]^+$ isomers produced initially can be calculated, and the relevant values are given in Table XI. It is clear from inspection of the results in the table that the intramolecular addition reaction of $[Co(en)_2(maleato)]^+$ yields *mer*(5,5)-$[Co(en)(aea)]^+$ as the predominant product (>90%) in both liquid NH_3 and Me_2SO. The proportion of *fac*(5,5)-$[Co(en)(aea)]^+$ produced in the reaction is higher in Me_2SO (9.5%) than in liquid NH_3 (3.7%).

Equilibration of $[Co(en)(aea)]^+$ Isomers with Activated Charcoal. Much evidence has established that activated charcoal assists the equilibration of a wide range of Co(III) amine systems.[44] Optically active $(-)_{589}$-Δ-*fac*(5,5)-$[Co(en)(R\text{-}aea)]ClO_4$ was equilibrated in water at 80 °C with activated charcoal present. When equilibrium was attained, the products were separated by chromatography. Three bands emerged, two of which were minor. The eluate of the main band was collected and analyzed for Co by AAS, and the CD spectrum was recorded. Similar equilibration and analysis procedures were carried out with $(-)_{589}$-*mer*(5,5)-$[Co(en)(aea)]ClO_4$, which was hydrolyzed in situ before charcoal was added, and $(-)_{589}$-*mer*(5,5)-$[Co(en)(aea)]ClO_4$, which was used directly. In order to determine the ratio between the *mer*(5,5)- and *fac*(5,5)-isomers of the main band from the chromatographic separation, the CD spectrum was analyzed as described above. Observed ΔA_λ values at selected wavelengths are given in the Supplementary Material (Table 27). When the same strategy as previously outlined is used, the mixtures were assumed to be composed of $(-)_{589}$-Λ-*mer*(5,5)-$[Co(en)(R\text{-}aea)]^+$ and $(-)_{589}$-Δ-*fac*(5,5)-$[Co(en)(R\text{-}aea)]^+$. Linear plots of $\Delta\epsilon(B/\lambda)/(\Delta\epsilon(A/\lambda) - \Delta\epsilon(B/\lambda))$ vs. $\Delta A_\lambda/(\Delta\epsilon(A/\lambda - \Delta\epsilon(B/\lambda))$ for different λ were obtained for each reactant isomer. Any other combination of the chiral *mer*(5,5)- and *fac*(5,5)-isomers did not give linear plots of this expression. The observed linearity indicates that only the $(-)_{589}$-Λ-*mer*(5,5)- and $(-)_{589}$-Δ-*fac*(5,5)-isomers of $[Co(en)(aea)]^+$ contribute to the CD of the mixtures. The total concentration of species contributing to the CD, as obtained from the slopes, and the fraction of $(-)_{589}$-*fac*(5,5)-$[Co(en)(aea)]^+$ isomer, as determined from the intercepts, are listed in Table XII. In all three experiments, the main component is the $(-)_{589}$-Δ-*fac*(5,5)-$[Co(en)(aea)]^+$ isomer with the $(-)_{589}$-Λ-*mer*(5,5)-$[Co(en)(aea)]^+$ isomer constituting less than 5% of the equilibrated mixture at 80 °C.

The Co concentrations measured by AAS are in two cases slightly higher than the concentrations of chiral components as obtained independently from the analyses of the CD spectra. This fact may signify a small (<14%) degree of racemization of the chiral aea ligand in the rather stringent conditions (80 °C) required to attain equilibrium reasonably fast. As outlined in the introduction the chirality of the quadridentate aea ligand governs the chirality of the complex. Therefore, if the racemization of the complexes has occurred, this must inevitably have involved racemization of the aea ligand as well. However, the results indicate enantiomeric excesses of no less than 87% in all instances. The isomer $(-)_{589}$-*mer*(5,5)-$[Co(en)(aea)]^+$ equilibrates to give es-

(44) Hammershøi, A.; Larsen, E. *Acta Chem. Scand. Ser. A.* **1978**, *32*, 485–491 and references therein.

Table XII. Product Distributions from Activated Charcoal Equilibration Experiments at 80 °C

	reagent complex		
	$(-)_{589}$-*fac*(5,5)-[Co(en)(aea)]$^+$	$(-)_{589}$-*mer*(5,5)-[Co(en)(aea)]$^+$	base-hydrolyzed $(-)_{589}$-*mer*(5,5)-[Co(en)(aea)]$^+$
$(-)_{589}$-*fac*(5,5)-[Co(en)(aea)]$^+$, as percentage of chiral species in mixture	95	>96	96
concn of $(-)_{589}$-*fac*(5,5)- and $(-)_{589}$-*mer*(5,5)-[Co(en)(aea)]$^+$ isomers, from "CD-plot" (mM)	1.86 (2)	2.7 (2)	1.62 (1)
Co concn, from AAS (mM)	1.92	2.56	1.85

sentially $(-)_{589}$-Δ-*fac*(5,5)-[Co(en)(*R*-aea)]$^+$. The chirality of the *N*-(2-aminoethyl)aspartate ligand must therefore be the same in both complexes, namely (*R*).

In a separate equilibration experiment $(-)_{589}$-*mer*(5,5)-[Co(en)(aea)]$^+$ was first hydrolyzed in 2 M NaOH for 35 min before treatment with activated charcoal in neutral solution. The equilibrated mixture had essentially the same composition with respect to chiral isomers as the mixture obtained from equilibration of $(-)_{589}$-*mer*(5,5)-[Co(en)(aea)]$^+$ directly. This result implies that no inversion of the asymmetric carbon atom in the aea ligand takes place in the course of the base hydrolysis reaction.

Discussion

The [Co(en)$_2$(maleato)]$^+$ Complex. Only a few Co(III) complexes containing isolated seven-membered chelate rings have been reported before.[45] In one paper from 1921, Duff[13] claims a number of [bis(ethylenediamine)]cobalt(III) complexes containing chelated dicarboxylates such as succinate, maleate, *meso*-2,3-dibromosuccinate, *meso*-tartrate, itaconate, or citraconate. In each of these complexes the dicarboxylato ligand was assumed to bind to the metal ion as a bidentate forming a seven-membered chelate ring. However, no conclusive evidence, by modern standards, was presented in support of this assertion. More recently, Carunchio and co-workers[46] demonstrated that chelated dicarboxylato complexes are in fact formed when Duff's procedure was repeated for the succinato and maleato complexes, albeit in far from quantitative yields. The X-ray crystallographic results reported in this study conclusively confirm the tris-bidentate nature of the [Co(en)$_2$(maleato)]$^+$ ion (Figure 3a).

Carunchio et al.[46] characterized the separated products formed in the reaction of [Co(en)$_2$(CO$_3$)]$^+$ with maleic acid on the basis of their absorption spectra. Apart from the chelated maleato complex, they observed substantial amounts of *trans*-[Co(en)$_2$(H$_2$O)(maleato)]$^+$ byproduct. On this basis it was proposed that the reaction of [Co(en)$_2$(CO$_3$)]$^+$ with the dicarboxylic acid yields a mixture of *cis*- and *trans*-[Co(en)$_2$(H$_2$O)(maleato)]$^+$. Of these isomers only the cis compound was assumed to form the chelated maleato complex by ring-closure, whereas the trans isomer could not do so directly but would need to isomerize first to the cis isomer. However, several possibilities for the mechanism of the cyclization may be visualized. These include carboxylate assisted removal of H$_2$O at the metal center or capture of carboxylate ion by a five-coordinate intermediate (S_N1 mechanism). Another possibility would be nucleophilic attack of coordinated H$_2$O (or OH$^-$) on the carboxylate ion in *cis*-[Co(en)$_2$(H$_2$O)(maleato)]$^+$. The last mechanism has been substantiated for the cyclization of N-bound glycine.[47]

If an analogous mechanism were to apply in the formation of chelated maleate from [Co(en)$_2$(H$_2$O)(maleato)]$^+$, only the cis isomer would lead to the cyclized product. Clearly, the coordinated OH$^-$ or H$_2$O nucleophile of *trans*-[Co(en)$_2$(H$_2$O)(maleato)]$^+$ cannot approach the uncoordinated carboxyl group for intramolecular ring closing. The relatively low yields of [Co(en)$_2$(maleato)]$^+$ produced in the Duff process may therefore be rationalized.

An alternative synthetic route involves reaction of *cis*-[Co(en)$_2$Cl$_2$]NO$_3$ with disilver maleate in CH$_3$OH and is reported to give almost quantitative yields of [Co(en)$_2$(maleato)]NO$_3$.[46] However, considering the low cost, ease, and reproducibility of Duff's original method, the yield of ~20% was sufficient for the present purposes.

The [Co(en)(aea)]$^+$ Isomers. (a) Structure. Complexes of Co(III) with the ligand aea have not been reported in the literature. The formation of a complex between Cu(II) and the ligand in solution has been suggested on the basis of thermodynamic evidence,[48] but no structural information was obtained. When aea functions as a quadridentate ligand in [Co(en)(aea)]$^+$, two topological isomers, *fac*(5,5) or *mer*(5,5), are possible as illustrated earlier (Figure 1). The *fac*(5,5)-[Co(en)(aea)]$^+$ isomer was identified by X-ray crystallographic techniques (Figure 3b). This isomer is the principal product in water after equilibration in the presence of activated charcoal, and at 80 °C it constitutes ~96% of the equilibrium mixture.

The reactions of [Co(en)$_2$(maleato)]ClO$_4$ with bases in liquid NH$_3$ or Me$_2$SO afforded a new complex. This had the same empirical formula as *fac*(5,5)-[Co(en)(aea)]ClO$_4$ and [Co(en)$_2$(maleato)]ClO$_4$, but revealed physical properties significantly different from those of these two compounds. The new species was attributed to the *mer*(5,5)-[Co(en)(aea)]$^+$ structure on the following basis.

Treatment of the *mer*(5,5)-[Co(en)(aea)]$^+$ ion with aqueous base afforded *mer*(5,5)-[Co(en)(aea)(OH)] with retention of the *mer*(5,5) arrangement of the aea ligand. Moreover, equilibration of the chiral *mer*(5,5)-[Co(en)(aea)]$^+$ isomer at 80 °C in the presence of activated charcoal resulted in a mixture containing >96% of the corresponding chiral *fac*(5,5)-[Co(en)(aea)]$^+$ complex (enantiomeric excess >87%). While *mer*(5,5)- and/or *fac*(5,5)-[Co(en)(aea)]$^+$ were readily separated from the related ions [Co(en)$_2$(maleato)]$^+$ and *mer*(5,5)-[Co(en)(aea)(H$_2$O)]$^+$ by chromatographic procedures, no separation of the two isomers themselves was achieved other than by crystallization and their reactivity toward OH$^-$. This would seem to be consistent with very similar outer-sphere solvation and ion-association characteristics of the two species, as might be expected for isomers of [Co(en)(aea)]$^+$. Both isomers have very similar, although not identical, absorption spectra, but their chiral forms display distinctly different and complex RD and CD spectra (Figure 2). Likewise, the ^{13}C NMR spectra (Figure 7) are demonstrably different but still very similar. The ^{1}H NMR spectra (not reported) were also different but too complex to be structurally revealing. All the evidence is consistent with the structural assignment for *mer*(5,5)-[Co(en)(aea)]$^+$.

(b) Relative Stability. The *fac*(5,5)-[Co(en)(aea)]$^+$ isomer is thermodynamically favored over the corresponding *mer*(5,5)-isomer. At 80 °C the proportion of the *fac*(5,5)-isomer was >96%. Such stereospecificity in the coordination of the aea ligand agrees qualitatively with results from analogous systems. The qua-

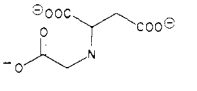

4

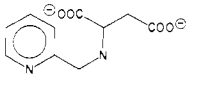

5

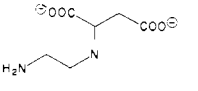

6

(45) Sato, S.; Saito, Y. *Acta Crystallogr., Sect. B.* **1975**, *31*, 1378–1381.
(46) Carunchio, V.; Grassini-Strazza, G.; Messina, A.; Prosperi, T. *Ann. Chim. (Rome)* **1974**, *64*, 257–264.
(47) Buckingham, D. A. In "Biological Aspects of Inorganic Chemistry"; Dolphin, D., Ed.; Wiley: 1977, and references therein.
(48) Courtney, R. C.; Gustafson, R. L.; Westerback, S. J.; Hyytiainen, H.; Chaberek, S. C., Jr.; Martell, A. E. *J. Am. Chem. Soc.* **1957**, *79*, 3030–3041.

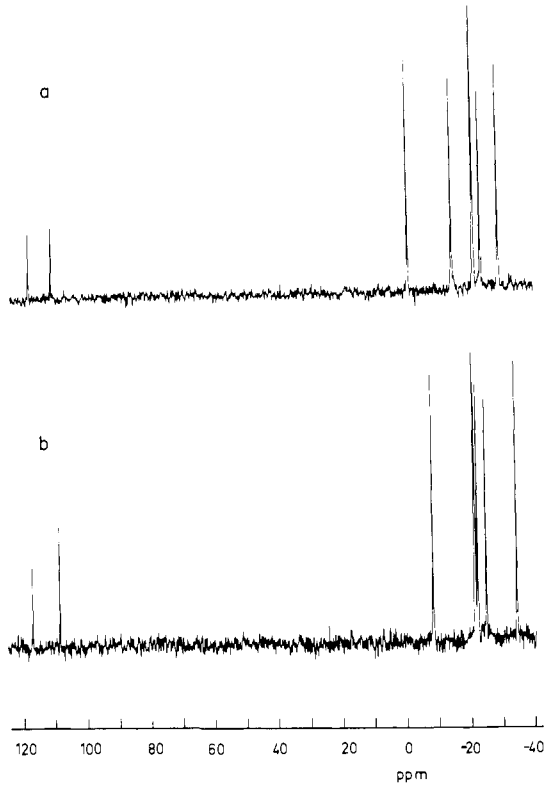

Figure 7. ^{13}C NMR spectra of *fac*(5,5)-[Co(en)(aea)]NO_3 (a) and *mer*(5,5)-[Co(en)(aea)]NO_3 (b) in D_2O.

dridentate ligands **4** and **5** are both structurally similar to aea, **6**, and would seem to be capable of coordinating to four sites on Co(III), in both a *mer*(5,5) and a *fac*(5,5) fashion. The Co(III) complexes of **4** and **5** (with chelated amino acidates occupying the remaining two coordination sites) have been synthesized and characterized. In both instances, the *fac*(5,5) isomers **7**, **8**,[49] and **9**[50] were obtained. The identities of **7** and **8** were proposed on

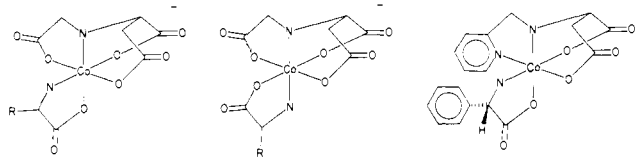

7 **8** **9**

the basis of their absorption, CD, and ^1H NMR spectra,[49] and the structure of **9** was elucidated by X-ray crystallographic analysis.[50] In no case were quadridentate "*mer*(5,5)-complexes" detected. However, the presence of small amounts of such isomers cannot be excluded, recalling the unsuccessful attempts at chromatographically separating the *mer*(5,5)- and *fac*(5,5)-[Co(en)(aea)]$^+$ isomers. A general trend regarding the favored geometry of these systems thus has emerged.

Theoretically, the preference for the *fac*(5,5) arrangement over the *mer*(5,5) arrangement has been rationalized in terms of the angular strain in the C–N–C angle centered on the secondary amine nitrogen atom. In the crystal structure of **9**, this angle (110.6 (6)°) was found to be very close to the ideal tetrahedral value of 109.5°, whereas the corresponding angle in the meridional situation was assumed to deviate from this value.[50] The corresponding angles (C2–N2–C5) in $(-)_{589}$-Δ-*fac*(5,5)-[Co(en)(*R*-aea)]$^+$ (112.9 (3)°) and in *mer*(5,5)-[Co(en)(aea)(H_2O)]$^+$ (116.7 (2)°) support this explanation. Although molecular mechanics energy minimization calculations may provide some quantitative information about the likely energy differences, they have not yet been carried out on this system.

Such calculations have recently been carried out for the two isomeric Co(III) complexes of (*S*,*S*)-ethylenediamine-*N*,*N*′-disuccinate, **10** and **11**.[51] The ligand can be regarded as being

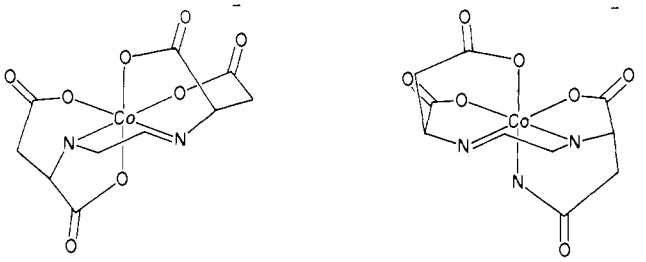

10 **11**

composed of two (*S*)-aspartate units linked together at the amino groups by an ethylene bridge. Isomer **10** corresponds to *fac*-(5,5)-[Co(en)(aea)]$^+$ with any one pair of adjacent five-membered chelate rings facially coordinated. Isomer **11** corresponds to *mer*(5,5)-[Co(en)(aea)]$^+$ with all five-membered chelate rings arranged meridionally. The calculation results indicate that **10** is more stable than **11** by ~6 kcal/mol.[51] This prediction is supported by an X-ray crystallographic analysis[35] of **10**, which was shown to be the sole isomer produced in solution.[52] According to the results of the energy minimization calculations, the higher energy of **11** arises most notably from the angle deformation energy of the C–N–C angle centered on the secondary amine nitrogen atom in **11**.[51] The calculated size of this angle is 111° in **10** and 119° in **11**. These calculated results for **10** and **11** parallel the corresponding values of 112.9 (3)° in *fac*(5,5)-[Co(en)(aea)]$^+$ and 116.7 (2)° in *mer*(5,5)-[Co(en)(aea)(H_2O)]$^+$ as found in the crystal structures.

(c) Reactions with OH^-. The two isomers of [Co(en)(aea)]$^+$ reveal distinctly different reactivity patterns with aqueous base. The *fac*(5,5)-[Co(en)(aea)]Br compound showed a complex dependence on [OH^-] with rate constants between 4×10^{-3} and 9×10^{-3} s^{-1} over the range from 0.025 to 1.0 M NaOH. The products were not identified, and it appeared that they readily reverted to the starting material on neutralization of the alkaline solution. No interpretation of the kinetic behavior of *fac*(5,5)-[Co(en)(aea)]$^+$ in terms of likely mechanisms will be attempted as the amount of available information is insufficient at this stage. Moreover, this information is not important for the present study since the rates are too slow to affect the understanding of the olefin reaction and subsequent complex chemistry.

The base-hydrolysis reaction of the *mer*(5,5)-[Co(en)(aea)]$^+$ isomer is much faster. It is a complicating feature of the reaction of the coordinated olefin and was therefore studied in detail. A summary of the experimental evidence is given below.

The structure of the ultimate product of the reaction is known (Figure 3c). The results of the charcoal-catalyzed equilibration experiments establish that the chiral C atom of the aea ligand retains its chirality throughout. The ^{13}C NMR spectra of the quenched reaction mixtures, coupled with the kinetic results, are consistent with two isomeric products, which arise by parallel reaction paths, each of which is first order in [OH^-]. In a subsequent reaction, one of these isomers is transformed to the other, which is the final product, and the rate of the isomerization reaction was independent of [OH^-] over the range from 0.025 to 0.20 M NaOH. A reaction scheme that accommodates all the evidence is proposed in Scheme I.

According to the proposal, *mer*(5,5)-[Co(en)(aea)]$^+$ (**3**) reacts with a molecule of OH^- in a rapid preequilibrium step producing the conjugate base **12**, which dissociates to a five-coordinate

(49) Colomb, G.; Bernauer, K. *Helv. Chim. Acta* **1977**, *60*, 459–467.
(50) Meiske, L. A.; Jacobson, R. A.; Angelici, R. J. *Inorg. Chem.* **1980**, *19*, 2028–2034.
(51) Pavelcik, F.; Majer, J. *Collect. Czech. Chem. Commun.* **1978**, *43*, 239–249.
(52) Neal, J.; Rose, N. J. *Inorg. Chem.* **1968**, *7*, 2405–2412; **1972**, *12*, 1226–1232.

Scheme I

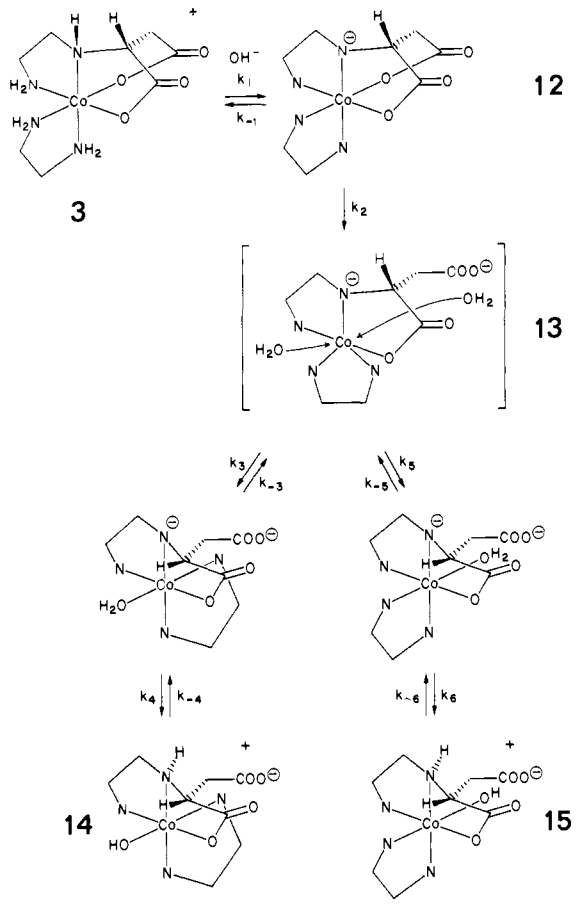

intermediate, idealized as **13**, by breaking a Co–O bond. This short-lived intermediate captures a molecule of water from the solvent. Depending on the direction from which this molecule approaches, two isomers **14** and **15** result. These isomers are similar to each other with respect to the bonding mode and conformational characteristics of the tridentate aea ligand and differ only in the position of the H_2O and en ligands on the metal relative to the aea ligand. Isomer **14** is that found in the crystal structure and is the exclusive end product of the overall reaction.

The two parallel reactions leading to **14** and **15** contribute in the ratio ~40:60. The presence of these parallel reactions strongly supports the involvement of the proposed five-coordinate intermediate **13** and would seem to preclude a mechanism which involves O–C bond rupture. The latter mechanism has been demonstrated[53] for the base hydrolysis of $[(H_3N)_5Co(OOCCF_3)]^{2+}$ and almost certainly applies to the base-catalyzed ring opening in $[Co(EDTA)]^-$.[54] Attack of OH^- on the coordinated carboxylato group is followed by O–C bond cleavage at the oxygen atom bound to the metal ion. The consequence is that the coordinated oxygen atom remains attached to the metal center, and the coordination geometry remains unaltered. If the base-hydrolysis reaction of *mer*(5,5)-$[Co(en)(aea)]^+$ (**3**) had proceeded by this mechanism, exclusively, only one isomer **15** would have been produced initially. The experiments do not rule out the "C–O bond fission" mechanism as a parallel route to isomer **15**, but it is excluded as a route to isomer **14**. Isotopic labeling studies would be required to settle this issue.

Evidence that H_2O, and not OH^-, is the species captured by the intermediate **13** in such conjugate base hydrolyses is provided by $^{18}OH_2/^{16}OH_2$[55] and anion[56] competition studies for the base hydrolysis of a series of acidopentaaminecobalt(III) complexes.

The transformation of **15** to give **14** was found to be independent of the hydroxide ion concentration ($k = 0.05\ s^{-1}$). Either base-independent OH^- exchange at the complex or OH^--catalyzed H_2O exchange arising from the hydroxo complex would accommodate this base-independent isomerization. An intramolecular rearrangement process is difficult to imagine because of the meridional coordination mode of the aea ligand in the complexes **14** and **15**, and base-independent OH^- exchange seems very unlikely also.[55] The water exchange path could arise from abstraction of a proton on one of the amine centers by the coordinated OH^-. The generated aminato ion thereby labilizes the bound water molecule, and overall the reaction would be independent of OH^-, at least in near neutral conditions. Labeling studies might eliminate the intramolecular path but could not distinguish between the other two paths. The case has been argued for OH^--catalyzed H_2O exchange in order to be consistent with the path for H_2O capture by the conjugate base **13**. Water exchange alone in the aqua complex is too slow to accommodate the results (no change of ^{13}C NMR spectrum over 17 h at pD ~1.5) and would inevitably depend inversely on $[OH^-]$ for the hydroxo substrate.

Like *mer*(5,5)-$[Co(en)(aea)]^+$ (**3**), the end product **14** of the reaction incorporates the meridional arrangement of two linked five-membered chelate rings that share a coordinated secondary amine group. The three ligating atoms of this arrangement are, therefore, most likely to have remained essentially fixed in their positions relative to each other and the metal ion. As is typical for such a system,[57] the conformations of the two five-membered chelate rings in **14** are interlocked. Since the tridentate ligand remains coordinated to the metal at all points, inversion of the conformations of the two linked chelate rings can only take place simultaneously and if the secondary amine donor also inverts its configuration. Since the amine is coordinated with the electron lone pair to the metal center by a kinetically inert bond, such inversion can take place only if the amine is deprotonated.[58] This would have been possible under the alkaline conditions of the reaction and is implied by the mechanism depicted in Scheme I.

In the solid-state structure of **14** (Figure 3), the free (dangling) carboxylatomethyl group is oriented with the C2–C3 bond equatorial to the chelate ring on which it is a substituent. It is also likely that the same conformations apply for the deprotonated complexes derived from the intermediate **13**. This conformation is presumably trapped by protonation of the secondary aminato group to give both **14** and **15** with common tridentate configurations and conformations. Since this tridentate configuration is thermodynamically stable in **14** we presume the same is also true for **15**.

The base hydrolysis reaction could also be initiated by deprotonation at one of the primary amine sites. If this applies, additional steps need to be incorporated in the scheme to accommodate the inversion at the secondary amine center and the concomitant conformational changes, at least for **14**.

The much greater reactivity with base of the *mer*(5,5)-$[Co(en)(aea)]^+$ complex in comparison with the *fac*(5,5)-$[Co(en)(aea)]^+$ isomer is striking. The ring opening of *mer*(5,5)-$[Co(en)(aea)]^+$, which takes place in the reaction, may help to relieve some of the strain energy of the C–N–C angle centered on the secondary amine donor. However, some deformation of this angle was still apparent in the crystal structure of the final product, *mer*(5,5)-$[Co(en)(aea)(H_2O)]^+$. Therefore other explanations for the difference in reactivity may be necessary.

The Mechanism of the Reaction of $[Co(en)_2(maleato)]^+$ and OH^-. Of the two possible isomers arising from the base-catalyzed intramolecular addition reaction of $[Co(en)_2(maleato)]^+$, the *mer*(5,5)-$[Co(en)(aea)]^+$ complex is the favored product in all three solvents investigated (H_2O, Me_2SO, and liquid NH_3). This specificity clearly calls for some comment.

(53) Jordan, R. B.; Taube, H. *J. Am. Chem. Soc.* **1966**, *88*, 4406–4410.
(54) Busch, D. H. In "Advances in the Chemistry of the Coordination Compounds"; Kirschner, S., Ed.; Macmillan: New York, 1961; pp 139–155.
(55) Green, M.; Taube, H. *Inorg. Chem.* **1963**, *2*, 948–950.
(56) Buckingham, D. A.; Olsen, I. I.; Sargeson, A. M. *J. Am. Chem. Soc.* **1966**, *88*, 5443–5447.
(57) Keene, F. R.; Searle, G. H. *Inorg. Chem.* **1972**, *11*, 148–156.
(58) Jackson, W. G.; Sargeson, A. M. In "Rearrangements in Ground and Excited States"; de Mayo, P., Ed.; Academic Press: New York, 1980; Vol. 1, Chapter 11 and references therein.

Scheme II

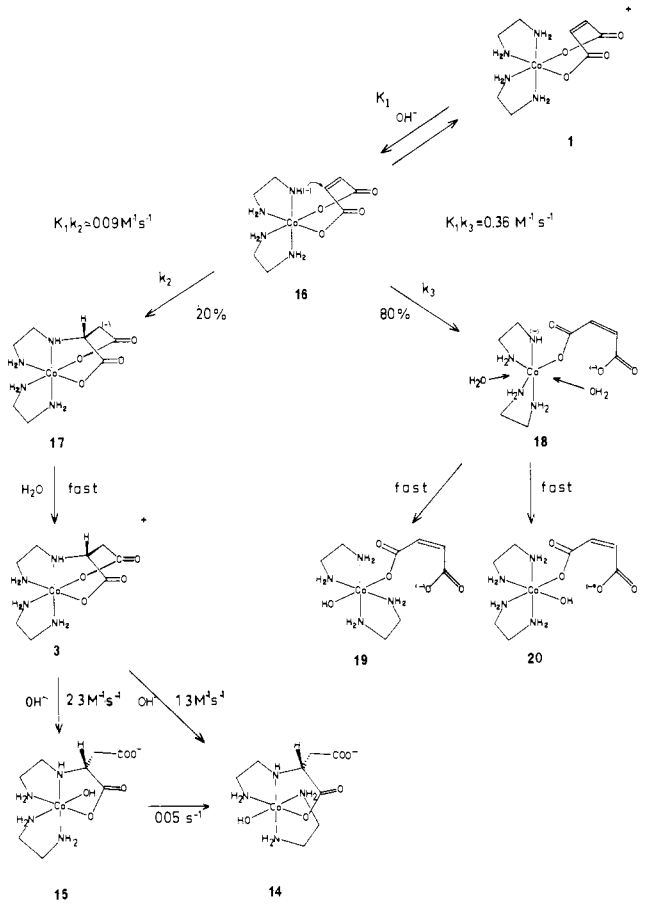

(a) Aqueous System. The kinetics of the reaction of $[Co(en)_2(maleato)]^+$ with OH^- display a rate law first order in $[OH^-]$ yielding the following products, *mer*(5,5)-$[Co(en)(aea)(OH)]$, *cis*- and *trans*-$[Co(en)_2(OH)(maleato)]$, and $[Co(en)_2(OH)_2]^+$. Of these products the proportion of *mer*(5,5)-$[Co(en)(aea)(OH)]$ present was independent of $[OH^-]$ and reaction time. A reaction scheme consistent with the observations is set out in Scheme II.

In a preequilibrium step, $[Co(en)_2(maleato)]^+$ (**1**) is deprotonated by OH^- to form the conjugate base **16**. If the coordinated aminato nucleophile is within a suitable distance from the maleate C–C double bond, nucleophilic attack at this site may occur to form **17** in a rate-determining step ($K_1k_2 = 0.09\ M^{-1}\ s^{-1}$). The carbanion **17** so generated rapidly captures a proton from the solvent producing *mer*(5,5)-$[Co(en)(aea)]^+$ (**3**), which in the alkaline conditions rapidly hydrolyzes ($k = 3.6\ M^{-1}\ s^{-1}$) according to the mechanism in Scheme I. Another reaction path involves ring opening of the maleate chelate (with Co–O bond fission), as a rate-determining step ($K_1k_3 = 0.36\ M^{-1}\ s^{-1}$), to produce a short-lived five-coordinate intermediate, idealized as **18**, which immediately reacts with a molecule of H_2O from the solvent. Depending on the direction of entry for this water molecule, both the *trans*- and *cis*-$[Co(en)_2(OH)(maleato)]$ complexes, **19** and **20**, result. These slowly hydrolyze to *cis*- and *trans*-$[Co(en)_2(OH)_2]^+$ (<4%).

As already argued, the product *mer*(5,5)-$[Co(en)(aea)(OH)]$ (**14**) is almost certainly produced by way of **3**. The *fac*(5,5)-$[Co(en)(aea)]^+$ complex (which would have appeared as a single band in the chromatographic product separation) was not observed (<1%). If it had been produced, it would not have reacted further under the conditions. The *mer*(5,5)-$[Co(en)(aea)]^+$ isomer is therefore the exclusive addition product in the aqueous system. The complex **14** does not arise from *cis*-$[Co(en)_2(OH)(maleato)]$.[10] Clearly the proportion of *mer*(5,5)-$[Co(en)(aea)(H_2O)]^+$ among the products was the same after $10t_{1/2}$ as after $t_{1/2}$ (Table X), and significant amounts of *cis*-$[Co(en)_2(H_2O)(maleato)]^+$ were present at both times. In summary, the intramolecular reaction leading to **3** (and subsequently **14**) therefore involves attack of deprotonated ethylenediamine on the maleate dianion, while the latter is coordinated as a bidentate ligand in **16** and stereoselectively at one olefinic C atom.

In Scheme II the addition of the aminato ion (**16** → **17**) is proposed as the rate-determining step. The carbanion so produced is presumably rapidly protonated since no general acid catalysis was observed for this process using buffer acids much more acidic than H_2O and the product. Such catalysis has been observed in an analogous intramolecular cyclization involving OH^- in *cis*-$[(en)_2Co(OH)(OOCC{=}CCOOCH_3)]^+$[59] where protonation is rate determining.

The carbanion produced by addition of the aminato ion to the chelated maleate cannot undergo rotation about the C–C bond since it is tied as a chelate, but it could invert at the β-carbon or it could delocalize over the oxygen atoms. Either of the latter two processes would account for the lack of specificity for the protonation at the β-carbon site. However, it is unlikely that the inversion rate would be fast compared with the expected diffusion-controlled protonation at the β-carbon center ($pK_a > 14$). Delocalization of the anion over the carboxylate group and deuteration with D_2O on either side of the planar entity would yield both diastereoisomers. This is the most likely explanation for the lack of specificity in the protonation step.

An approximate value for k_2 of the cyclization step can be deduced if an estimate of K_1 is made. From indirect evidence, pK_a values for Co(III)-coordinated amines are estimated to fall in the range 15–17 depending on the amine and the overall charge of the Co(III) complex.[60,61] The pK_a value for the relevant amine group in **1** (1+ ion) would be expected to fall in the upper region of the range. Clearly, from Scheme II, $K_1 = K_aK_w^{-1}$, and taking $pK_a \sim 17$ and $pK_w = 13.77$ (25 °C, $\mu = 1.0$ M) we obtain a rate-constant estimate $k_2 \sim 10^2\ s^{-1}$ for the cyclization step. This value is consistent with the observed value of $k = 67\ s^{-1}$ (25 °C, $\mu = 1.0$ M)[10] found for a related cyclization reaction of **21** to give **22**. It would also imply that binding both carboxylate groups

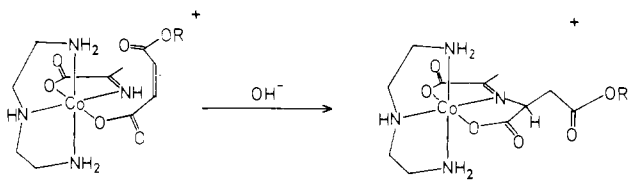

21 **22**

to the metal activates the olefin double bond to a degree similar to that caused by the pendant methoxycarbonyl group in the monodentate situation.

The occurrence of the ring-opening path leading to **19** and **20** is not surprising. The rate constant ($k = 0.36\ M^{-1}\ s^{-1}$ (25 °C)) is only ten times greater than that for the first base-hydrolysis step of *cis*-$[Co(en)_2(OOCCH_3)_2]^+$ ($k = 0.024\ M^{-1}\ s^{-1}$)[41] and the strain in the seven-membered chelate ring could readily account for the difference. A more surprising fact was that no intermolecular attack of OH^- on the olefinic bond in **1** (to produce $[Co(en)_2(maleato)]^+$) was observed. Probably the intramolecular addition reaction competes more than favorably with the intermolecular process, even allowing for the difference in the total concentrations of the nucleophiles.

(b) Nonaqueous Systems. No kinetic studies of the base-catalyzed reaction of $[Co(en)_2(maleato)]ClO_4$ in Me_2SO or liquid NH_3 were carried out. In these solvents, competing solvolysis reactions were absent and the intramolecular addition reaction occurred almost quantitatively. Notably, the *mer*(5,5)-$[Co(en)(aea)]^+$ isomer was the principal product but modest amounts

(59) Gahan, L. R.; Harrowfield, J. MacB.; Herlt, A. J.; Lindoy, L. F.; Sargeson, A. M.; Whimp, P. O., unpublished results.
(60) Creswell, P. J. Ph.D. Thesis, The Australian National University, 1974.
(61) Basolo, F.; Pearson, R. G. "Mechanisms of Inorganic Reactions", 2nd ed.; Wiley: New York, 1967; p 185.

of the *fac*(5,5)-isomer were also formed (<10%). The production of some *mer*(5,5)-$[Co(en)(aea)(H_2O)]^+$ was ascribed to hydrolysis in the not strictly anhydrous solvents or during the "workup".

When $(+)_{589}$-Λ-$[Co(en)_2(maleato)]ClO_4$ was the substrate, mixtures of optically pure $(+)_{589}$-Λ-*fac*(5,5)-$[Co(en)(S\text{-aea})]^+$ and $(-)_{589}$-Λ-*mer*(5,5)-$[Co(en)(R\text{-aea})]^+$ resulted for both Me_2SO and liquid NH_3. It is presumed that the intramolecular reaction occurs essentially by the same type of path as in the aqueous case. A base removes a proton from the coordinated ethylenediamine and the resultant aminato ion attacks the olefin. Subsequently or concertedly, the solvent or the conjugate acid of the base catalyst adds a proton to the carbon atom in the β-position to the site of attack. This proton capture was not stereospecific either.

By analogy with the aqueous system (Scheme II), the addition reaction takes place at the maleate ligand while it is bound to the metal ion at both ends. This is clearly the case, since the reaction takes place without any detectable isomerization around the metal center, and the absolute configuration of the reactant is preserved in the products. If the maleate chelate ring opened (with Co–O bond cleavage) prior to being attacked by the nucleophile and subsequently closed again, partial racemization of the products would have been expected.

Stereospecificity of the Addition Reaction. The *mer*(5,5)-$[Co(en)(aea)]^+$ isomer is preferred over the *fac*(5,5) isomer in the addition reaction in all three different solvents. This would seem to imply that the stereospecificity is a consequence of the structure of the chiral $[Co(en)_2(maleato)]^+$ reactant and is not critically solvent dependent. However, it should be emphasized that the product ratios of 96:4 and 90:10 in liquid NH_3 and Me_2SO, respectively, correspond to small energy differences of ~1.5 kcal/mol. Hence, the observed stereospecificity may be decided by rather subtle effects. Some of the factors that may be important are discussed below.

One of the interesting features of the Λ-$[Co(en)_2(maleato)]^+$ ion in the solid-state structure (Figure 3a) is that the maleate chelate ring adopts a pseudoboat conformation that places the olefin carbon atoms C2 and C3 into close proximity to N2. Intramolecular addition of the amine group to the double bond with attack by N2 at C2 would produce Λ-*fac*(5,5)-$[Co(en)(S\text{-aea})]^+$, while attack at C3 would yield Λ-*mer*(5,5)-$[Co(en)(R\text{-aea})]^+$. This conformation of the maleate ring does not favor attack at any one of the olefin carbon atoms over the other. N2 is essentially equidistant from the two atoms and each carboxylate group and the olefin plane are far from being coplanar. However, the structural information indicates that the maleate chelate ring is able to attain a conformation that brings the olefinic carbon atoms into reasonable proximity to a coordiated aminato group. The conformation found in the crystal does not necessarily apply in solution, nor is it necessarily retained in the transition state. In fact, the ^1H and ^{13}C NMR spectra of $[Co(en)_2(maleato)]^+$ imply a degree of conformational flexibility, which causes the olefinic protons and carbon atoms, respectively, to become mutually equivalent on the NMR time scales involved.

From an examination of a Dreiding model of $[Co(en)_2(maleato)]^+$ it is evident that this conformational flexibility allows coplanarity to be achieved between the π-systems of the olefin moiety and one coordinated carboxylate group but not with both carboxylate groups at the same time. According to the general organic lore, such coplanarity should optimize the susceptibility of the olefin to attack by a nucleophile. Of course coplanarity is not mandatory but desirable since the activation by conjugation should fall off as a function of cos 2θ, where θ is the dihedral angle between the planes of the π-systems of the olefin and the $-COO^-$ group. A balanced compromise between this and other steric requirements, such as a sufficiently short distance between the reacting centers, may obtain.

When averaged over its possible conformations, the maleate chelate ring is symmetrical. Therefore, it might be expected that the selectivity of the intramolecular addition reaction is linked with the possible orientations of the electron lone pair on the coordinated aminato nucleophile. These orientations are decided by the conformations of the ethylenediamine chelate ring of which the nucleophile is part. Inspection of a Dreiding model reveals that when the en chelate ring is in the "ob" conformation (**23**), the direction of the lone pair essentially bisects the maleate bite angle, and there is no apparent preference from this source. In

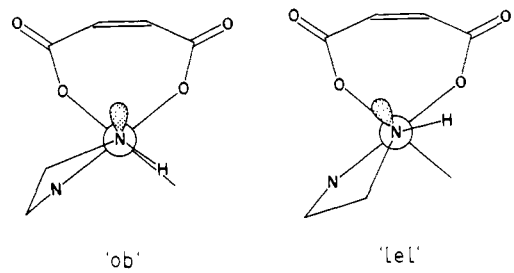

23 **24**

the "lel" conformation (**24**), the lone pair clearly has little proximity to either C atom and is unlikely to be effective. It is anticipated, therefore, that a complex interplay of several geometrical factors in the transition state is responsible for the observed stereospecificity of the addition reaction. In a general way, it could be argued that the nucleophile adds to the center of the olefin, and the configuration that the carbanion transition state experiences first, as it decays, is that of the least stable isomer (*mer*(5,5)-$[Co(en)(aea)]^+$), which is trapped by protonation before it reaches the more stable *fac*(5,5) configuration.

Some Implications of This Study. It has been established here that the maleate dianion, when bound as a bidentate to a metal center (in this case Co(III)), is susceptible to intramolecular nucleophilic attack, at least by a coordinated aminate ion. By analogy, coordinated *cis*-aconitate dianion should also be able to react in this way, as assumed in Glusker's proposal for the mechanism of aconitase.[7] For practical reasons, coordinated aminate was the nucleophile in the present study, but OH^-, which would be regarded as an inferior nucleophile to the aminate ion, appears to be involved in the mechanism of aconitase. However, comparison of the results from other model-complex studies[59] with those of this study imply that coordinated OH^- should still be efficient as a nucleophile toward chelated maleate. This is concluded from the fact that coordinated OH^- was an efficient nucleophile[59] in the intramolecular addition to monodentate maleate monomethyl ester ($k \sim 0.05\ s^{-1}$), and the chelated maleate dianion showed essentially the same reactivity as the maleate monomethyl ester toward the aminato nucleophile.

Recently, evidence of iron–sulfur clusters in aconitase has been obtained, and it seems that the active form contains an Fe_4S_4 cluster.[62] In nearly all other proteins where such clusters have been identified, their functions have been related to oxidation–reduction processes.[63] The discovery of an iron–sulfur cluster in aconitase, an enzyme that has no known electron-transfer function, is therefore surprising, and its presence demands a reassessment of the role of the iron. The biochemical studies imply acid–base addition–elimination chemistry for the hydration–dehydration process rather than redox-radical chemistry, and the model chemistry implies that the rates could be fast enough if an Fe site bound the substrate and also provided a coordinated OH^- ion. The role of the redox cluster could be to regulate the enzyme by switching it on or off. It is not likely that an iron atom in the Fe_4S_4 cluster binds both OH^- and the substrate. It seems more likely that a separate iron atom in the enzyme conducts the chemistry consistent with the NMR studies[6] or that hydration of aconitic acid occurs without the direct involvement of a metal ion, which is inconsistent with the NMR studies.[6] More speculation seems unwarranted at this stage, and an X-ray crystallographic analysis of the enzyme with an inhibitor such as fluorcitrate is badly needed.

(62) Beinert, H.; Emptage, M. H.; Dreyer, J.-L.; Scott, R. A.; Hahn, J. E.; Hodgson, K.; Thomson, A. J. *Proc. Natl. Acad. Sci. U.S.A.* **1983**, *80*, 393 and references therein.

(63) Cammack, R. *Nature* (*London*) **1980**, *286*, 442.

The *N*-(2-aminoethyl)aspartic acid is an analogue of the aspergillomarasmins,[64] which are naturally occurring aspartic acid derivatives isolated from various fungi pathogenic toward higher plants. Recently, a new member, *N*-(2-amino-2-carboxyethyl)-aspartic acid was added to this group.[64] A high degree of specificity must be involved in the action of the aspergillomarasmines since systematically closely related plants have appeared to react differently toward the pure toxins.[64] In certain plants, the toxic effects are not seen unless iron is also present,[65] which may imply the involvement of iron complexes as the toxins in these plants. Analogues might also be active, and the demonstrated chelating ability of *N*-(2-aminoethyl)aspartic acid combined with its structural resemblance to *N*-(2-amino-2-carboxyethyl)aspartic acid therefore prompted the biological testing of the two isomers. However, so far no activity has been detected.[66]

Acknowledgment. We are grateful for generous allocations of time on the UNIVAC 1100/42 computer at the A.N.U. Computer Service Centre and for technical assistance provided by D. Bogsanyi, B. Fenning, C. H. Jacob, the R.S.C. NMR and Photographic Services Units, and the A.N.U. Microanalytical Service Unit.

(64) Bach, E.; Christensen, S.; Dalgaard, L.; Larsen, P. O.; Olsen, C. E.; Smedegaard-Petersen, V. *Physiol. Plant Pathol.* **1979**, *14*, 41-46 and references therein.
(65) Gaumann, E. In "Advance in Enzymology"; Nord, F. F., Ed.; Interscience: London, New York, 1951; Vol. XI, pp 401-435.
(66) Friis, P.; Olesen-Larsen, P.; unpublished results.

Registry No. 1, 89254-95-5; **1**·ClO_4, 89255-00-5; **1**·[Sb_2L_2] (L = (+)-tartrato), 89255-03-8; **2**, 89361-08-0; **2**·Br, 89255-08-3; **3**, 89361-10-4; I, 89254-97-7; II, 89198-00-5; III, 89254-99-9; OH^-, 14280-30-9; (−)-Δ-[$Co(en)_2L$]ClO_4 (L = maleato), 89255-02-7; *mer*(5,5)-[Co(en)(aea)]ClO_4, 89255-05-0; *mer*(5,5)-[Co(en)(aea)]NO_3, 89255-06-1; *mer*(5,5)-[Co(en)(aea)]O_3SCF_3, 89255-07-2; *mer*(5,5)-[Co(en)(OOCCH($NHCH_2CH_2NH_2$)CDHCOO)]O_3SCF_3, 89198-03-8; (−)-Δ-*fac*(5,5)-[Co(en)(aea)]Br, 89198-04-9; Δ-*fac*-[Co(en)(aea)]·ClO_4, 89198-05-0; *fc*(5,5)-[Co(en)(aea)]NO_3, 89255-10-7; aconitase, 9024-25-3; (+)-(*R*)-*N*-(2-aminoethyl)aspartic acid, 89198-06-1; (−)-(*S*)-*N*-(2-aminoethyl)aspartic acid, 89198-07-2.

Supplementary Material Available: A listing of anisotropic thermal parameters, structure factor amplitudes, results of least-squares mean planes calculations, bond lengths and angles for the anions, final atomic fractional coordinates and isotropic thermal parameters for the hydrogen atoms of Δ-*fac*(5,5)-[Co(en)(aea)]BCS·$3H_2O$ and [Co(en)(aea)(H_2O)]ClO_4·$2H_2O$, $\Delta\epsilon_\lambda$ values at selected wavelengths for chiral *mer*(5,5)-[Co(en)(aea)]$^+$ and *fac*(5,5)-[Co(en)(aea)]$^+$ and mixtures thereof from product distribution experiments, and an Appendix describing how the calculations for Figure 5 were carried out (59 pages). Ordering information is given on any current masthead page.

Finite and Infinite Ribbons: From Platinum Alkyne Complexes to Extended Structures of the K_2PtAs_2 Type

Dennis J. Underwood, Michael Nowak, and Roald Hoffmann*

Contribution from the Department of Chemistry, Cornell University, Ithaca, New York 14853.
Received June 17, 1983

Abstract: The band structure of $[PtAs_2^{2-}]_\infty$ is calculated and analyzed in terms of the increased stability afforded by bending the planar chain into the experimental "zig-zag" ribbon structure. The increasing band gap with increased bending is explained in terms of stabilizing and destabilizing various crystal orbitals as a result of avoided crossings. This bending becomes unfavorable due to Pt–Pt σ^* interactions at small angles. Molecular orbital calculations on D_{4h} $PtAs_4^{6-}$, the coordination unit of this chain, indicate that an e-set is half occupied. A Jahn–Teller active distortion is the D_{4h} to D_{2h} scissor motion resulting in a minimum in the total energy close to the angle observed in the chain. Complexes of the general type $Pt(RC_2R)L_2$ **3**, $Pt(RC_2R)_2$ **4**, $Pt_2(\mu\text{-}RC_2R)L_4$ **5**, $Pt_2(\mu\text{-}RC_2R)(R'C_2R)_2$ **6** and $Pt_3(\mu\text{-}RC_2R)_2L_4$, which can be considered as oligomers of the notional chain $[PtRC_2R]_\infty$, are also studied; in particular, the relationship between structures **3** and **4** and **5** and **6** is investigated. Further, the connection between these compounds and the chain is considered in terms of addition of $Pt(HC_2H)^{2-}$ units to a terminal alkyne ligand. The similarity between $[PtAs_2^{2-}]_\infty$ and $[PtHC_2H^{2-}]_\infty$ becomes more apparent as the isolobal relationship between As_2 and HC_2H is detailed. This relationship is further emphasized by the band structure of various model alkyne chains.

Introduction

There exists a series of compounds having the general stoichiometry A_2MX_2, where A is an alkali metal ion (K, Na, Rb), M is a transition metal ion from group 8 (Pd, Pt), and X is a main group 5 or 6 ion (P, As, S).[1] The extended structures represented by these stoichiometries have much in common but show distinct and regular variations on changing the electron count.

In general, the compounds K_2MX_2 (M = Pd or Pt and X = P or As) consist of infinite "zig-zag" ribbons of MX_2 units surrounded by a graphitic network of potassium ions.[1a,b] Figure 1 is a representation of the structure of K_2PdAs_2 showing the relationship between the extended chains and K^+ network.

In K_2PdAs_2 the As–As distance is 2.41 Å, and in the corresponding K_2PdP_2, P–P is 2.17 Å. These separations are typical of P–P or As–As single bonds.[2-4] The Pd–Pd distances are 3.01, indicating possibly some interaction, but less than a single bond.[5] The MX_2 ribbons are strongly "puckered" or nonplanar, as Figure 1 and the Pd-centroid As_2–Pd angle 87.0° indicates.

In contrast to these puckered one-dimensional chains **1** stands the K_2PtS_2 structure.[1c] This contains planar PtS_2 chains of type **2**. The distance between sulfurs within a PtS_2 unit is 3.06 Å, and that between adjacent units is 3.59 Å. This indicates little S–S

(1) (a) Schuster, H.-U.; Rősza, S. *Z. Naturforsch.* **1979**, *34b*, 1167-1168. (b) Rősza, S.; Schuster, H.-U. *Ibid.* **1981**, *36b*, 1666-1667. (c) Bronger, W.; Günther, O. *J. Less-Common Met.* **1972**, *27*, 73-79. (d) Bronger, W.; Günther, O.; Huster, J.; Spangenberg, M. *Ibid.* **1976**, *50*, 49-55.
(2) (a) Maxwell, L. R.; Hendricks, S. B.; Mosely, V. M. *J. Chem. Phys.* **1935**, *3*, 699-709. (b) Burns, J. H.; Waser, J. *J. Am. Chem. Soc.* **1957**, *79*, 859-865. (c) Hedberg, K.; Hughes, E. W.; Waser, J. *J. Acta Crystallogr.* **1961**, *14*, 369-374.
(3) (a) Faust, A. S.; Foster, M. S.; Dahl, L. F. *J. Am. Chem. Soc.* **1969**, *91*, 5633-5635. (b) Faust, A. S.; Campana, C. F.; Sinclair, J. D.; Dahl, L. F. *Inorg. Chem.* **1979**, *18*, 3047-3054.
(4) (a) *Chem. Soc. Spec. Publ.* **1965**, No. 18. (b) Campana, C. F.; Vixi-Orosz, A.; Palyi, G.; Markó, L.; Dahl, L. F. *Inorg. Chem.* **1979**, *18*, 3054-3059.
(5) Wells, A. F. "Structural Inorganic Chemistry", Clarendon Press: Oxford, 1975; p 1022.

0002-7863/84/1506-2837$01.50/0